

261°

OPTICAL FIBER ATTENUATION MEASUREMENT

OPTICAL FIBER ATTENUATION MEASUREMENT

By

GARY STEPHEN DUCK, B.Sc.

A Project

Submitted to the School of Graduate Studies

in Partial Fulfilment of the Requirements

for the Degree

Master of Engineering

McMaster University

1979

MASTER OF ENGINEERING (1979)

TITLE: Optical Fiber Attenuation
 Measurement

AUTHOR: Gary Stephen Duck, B.Sc. (Carleton University)

SUPERVISORS: Dr. J. Straus, Dr. F.D. King, Dr. J.P. Marton

NUMBER OF PAGES: ix, 58

A B S T R A C T

Optical fibers are becoming so good that their optical and mechanical properties are fast approaching fundamental limits. It has also become evident that there is a requirement for establishing accurate and precise measurement techniques of these properties. The optical loss is the most important parameter characterizing fiber. This project reviews the subject of loss (or attenuation), its measurement and some of its subtleties.

Presently at BNR there are two attenuation measurements made: (1) one is the LED steady-state attenuation at $\lambda \approx 840$ nm, which makes use of a "pigtail" launching fiber and (2) the second is the spectral attenuation from 600-1400 nm. Both measurement techniques were developed by the author and Dr. K. Abe during the summer work term and made considerable improvements in both accuracy and speed over previously established methods. Some of the subtleties of attenuation which were also studied during this period were the effects of different launch conditions, and environmental effects such as those caused by temperature and ice. The extensive temperature tests done on the fiber led to the change from "hytrel" and nylon as coating materials to the use of silicone (which is still in use at BNR).

Throughout the paper, results of the measurements have been given for several types of fibers because some of them have very unique characteristics and applications.

All of the data displayed for this project was gathered by the author unless otherwise noted.

ACKNOWLEDGEMENTS

I wish to thank Dave King of Dept. 3K20 and Josef Straus of Dept. 3K23 (Fiber Optics Components) for their help and advice during the project period. Very special thanks to K. Abe of Dept. 3K21 (Optical Fiber and Cable) who worked with me on several internal BNR memos throughout the summer and whose expert knowledge of the subject was indispensable.

I would also like to express my appreciation to some of my other co-workers, P. Garel-Jones, C.C. Tan and F.P. Kapron (Senior Scientist-Theoretician) who were always available for advice.

Finally, thanks to Chris Waterman (BNR) and Joy Brohman (BNR) for an excellent job of typing.

TABLE OF CONTENTS

ABSTRACT	iii
ACKNOWLEDGEMENTS	v
LIST OF ILLUSTRATIONS	viii
CHAPTER	
I INTRODUCTION	1
II OPTICAL FIBER SPECTRAL ATTENUATION	3
2.1 General Description	3
2.2 Measurement Description	6
2.2.1 Detectors	6
2.2.2 Direct Display of Spectral Attenuation	10
2.3 Examples of Spectral Attenuations	17
2.3.1 Phosphorus Doped Silica-Core Fibers	17
2.3.3 <u>Silicone-Cladded</u> Silica-Core Fibers	19
III ATTENUATION CONSIDERATIONS	23
3.1 Optical Power vs Length	23
3.1.1 General Description	23
3.1.2 <u>Silicone-Coated</u> Fibers	26
3.2 Launch Conditions	34
3.2.1 Attenuation vs Launching Numerical Aperture	34
3.2.2 Coupled Power from an LED	39
3.3 Environmental Dependence of Attenuation	40
3.3.1 Hytrel Coated Fibers	40
3.3.2 Silicone Coated Fibers	49
IV CONCLUSION	51

APPENDIX A

A Calculation of the Relative Amounts of Core and Cladding Light in a Silicone Coated Optical Fiber vs Fiber Length	52
---	----

APPENDIX B

A Calculation of the Light Collected by a Fiber from a Lambertian LED.	55
---	----

REFERENCES	57
------------	----

LIST OF ILLUSTRATIONS

FIGURE	PAGE
1. Spectral Attenuation of Low Loss Germanium Doped Fiber	4
2. Spectral Attenuation in dB/km/ppm of OH ⁻ in Fused Silica	5
3. Rayleigh Scattering	5
4. Relative Response vs Wavelength for Silicon and Germanium Detectors	9
5. Conventional Technique for Measuring Spectral Attenuation	11
6. New Measurement Setup for Spectral Attenuation	12
7. Spectral Attenuation Curve for 2.3 km Fiber Showing Large OH ⁻ Absorption Peaks	15
8. Graph of $\text{Log } \frac{I_S(\lambda)}{I_R(\lambda)}$	16
9. "W" Shaped Index Profile Fiber #288	18
10. Spectral Attenuation of P-Doped Silica Core B-Doped Cladding Fiber #288	18
11. Spectral Attenuation of Silanox-WF with Shin-Etsu 103 Silicone Cladding	21
12. Spectral Attenuation of Suprasil-2 with Shin-Etsu 103 Silicone Cladding	22
13. Output Power vs Length (Fiber #228)	24
14. Log (Output Power) vs Fiber Length (Fiber #288)	25
15. Spectral Loss of Unclad Fiber Made From Commercial-Grade T08.	28
16. Cladding Loss Measurement of Graded Index Fiber	29
17. Power vs Length - Silicone Coated Fiber (NT44)	30
18. LED Light Captured by Core and Cladding of a Silicone Coated Graded Index Fiber	32

FIGURE	PAGE
19(a) Video Link with Return Voice Down Cladding	35
19(b) Achievable Coupling Ratio's	35
20 Attenuation vs Launching N.A.	37
21(a) Attenuation vs Launching N.A. Setup	38
(b) Modal Dependence of Attenuation for Step Index Fiber	38
(c) Modal Dependence of Attenuation for Graded Index Fiber	38
22 Attenuation vs Temperature (Fiber #197,183m)	43
23 Attenuation vs Temperature (Fiber #198,485m)	44
24 Fiber Output vs Temperature Cycle	45
25 Attenuation vs Temperature for Cabled Fibers (530m)	47
26 Freeze Test, Duplex Cable	48
27 Attenuation vs Temperature of Silicone Coated Fiber	50

CHAPTER 1

INTRODUCTION

At BNR, the first measurement performed on a newly manufactured fiber is an attenuation measurement with a BNR LED source centered at $\lambda = 840$ nm. It is a meaningful measurement as it is done with the source that will be used for most applications and allows for a fast and accurate determination of the quality of the new fiber. The method used is the standard two point technique. This consists of first measuring the optical power emitted from the test fiber end then cutting the fiber at a short distance from the launch end and measuring the optical power at this point. The fiber loss is calculated from these powers. A steady-state mode exciter must be used as a source for this measurement (the reason for this is described in the section on "Optical Power vs Length" p. 23). BNR has chosen to use a "pigtail" fiber (to which the LED is attached) for this purpose. The accuracy of this measurement is ± 0.1 dB.

A loss spectrum measurement is also done on selected fibers generally for construction and maintenance purposes. Usually the amount of OH^- ions incorporated in the glass is under investigation when such a measurement is required. The technique explained in this project uses an optical fiber taper coupler to monitor both the output from the test fiber and the short length output (actually a constant times the short length reading) at the same time. The attenuation at the L.E.D. wavelength (already measured with the two point technique described above) is used to pin down the proportionality constant in the short

length reading, making it possible to display the fiber's spectral attenuation directly (see p. 10). This measurement technique is unique to BNR.

The remainder of the measurements described in Chapter 3, such as the dependence of attenuation on launching N.A. and temperature, are not routinely done but are kept for characterizing general fiber types. The effects of these parameters, however, must always be kept in mind.

CHAPTER 2
OPTICAL FIBER SPECTRAL ATTENUATION

2.1 General Description

A typical attenuation versus wavelength curve for a low loss germanium doped CVD made (chemical vapour deposition) fiber is shown in Figure 1. The regions of interest are the 800-900 nm and the 1100-1400 nm spectral bands. Material absorption losses in these regions are primarily the result of the presence of OH^- water ions and transition metal ions such as Fe^{2+} , Cu^{2+} , etc. The OH^- ion is generally believed to be incorporated into the silica network in the form of Si-OH bonds. It has a fundamental stretching vibration at $2.72 \mu\text{m}$ and its first overtone is at $1.37 \mu\text{m}$. There is also an absorption peak at $1.23 \mu\text{m}$ attributed to the combinational vibration of the second overtone with the fundamental SiO_4 tetrahedral vibration at $12.5 \mu\text{m}$. Figure 2 is a plot of the spectral absorptive attenuation of OH^- in fused silica.⁽¹⁾ The large peak at 950 nm is from the second overtone of the fundamental absorption peak of OH^- . The concentration of OH^- required to maintain the absorptive attenuation at 1 dB/km across the spectral band of interest (800-1300) nm is approximately 1 ppm.* The lowest OH^- content observed so far by the present technique is 50 ± 10 ppb.

Loss by material scattering in optical fibers is caused mainly by Rayleigh scattering which is a fundamental limitation of the material

* Barnoski and Personick, p. 430.

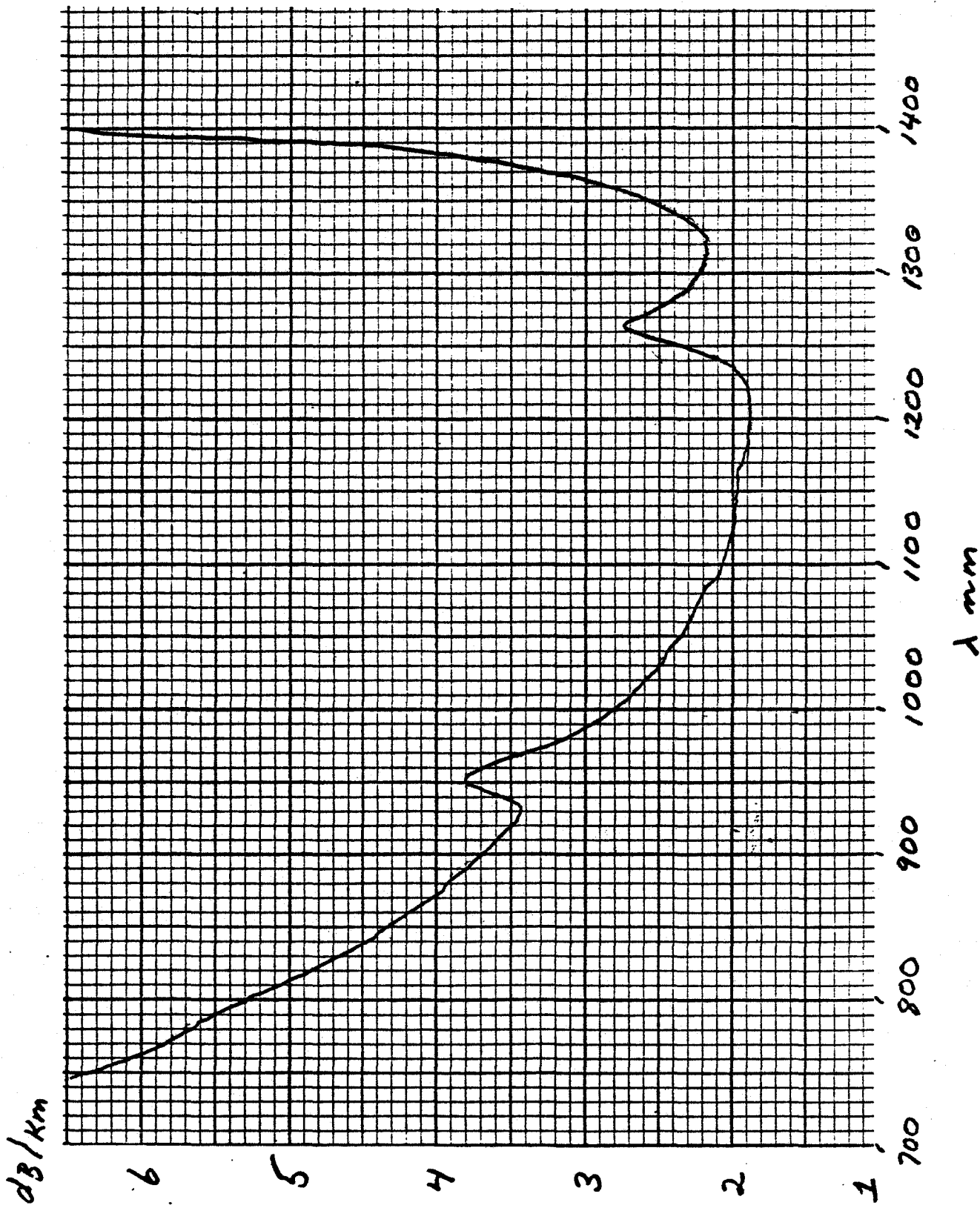


Fig. 1 SPECTRAL ATTENUATION OF LOW LOSS GERMANIUM DOPED FIBER

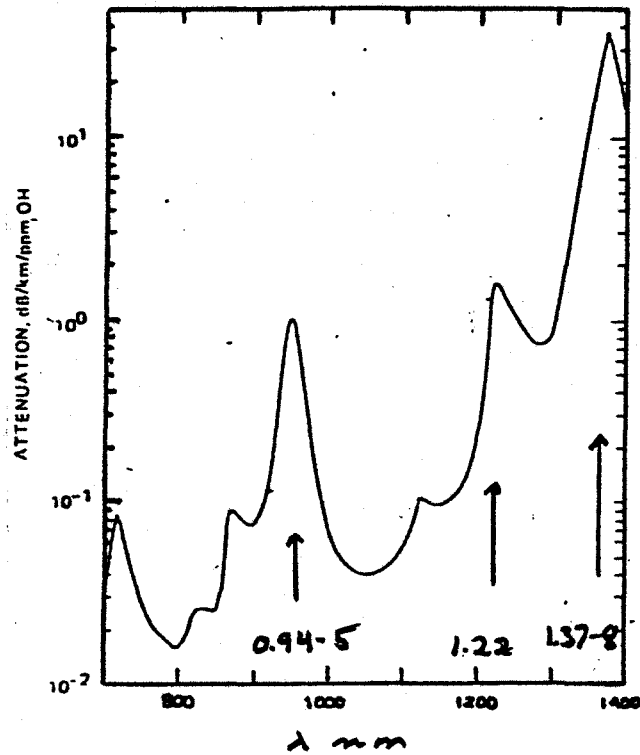


FIG. 2 SPECTRAL ATTENUATION IN dB/km/ppm of OH^- IN FUSED SILICA (AFTER BARNOWSKI ET AL [1])

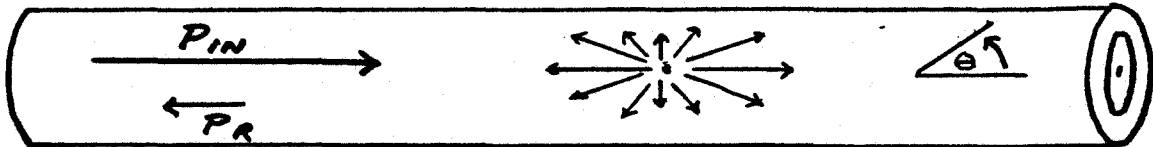


FIG. 3 RAYLEIGH SCATTERING
 - VARIES AS λ^{-4} and as $(1 + \cos^2 \theta)$
 - FOR DC SIGNALS

$$P_R \sim P_{IN} \frac{R^1}{\lambda^4} (NA)^2 (1 - e^{-2\alpha' L})$$

WHERE $\alpha' = 0.23 \times \text{dB/km}$

$R^1 \approx 0.59/\text{km} @ 0.85$

$L = \text{LENGTH IN KM}$

and cannot be prevented. It occurs when the scattering centers are considerably smaller than a wavelength of the incident light. The scattered photons retain their original energy (i.e. frequency) but are redirected into an angle θ (between the direction of observation and that of propagation of the incident photons) with a probability proportional to $(1 + \cos^2\theta)$ (Fig. 3). Total Rayleigh scattering loss depends on wavelength, varying as λ^{-4} , and on the numerical aperture of the fiber, varying as NA^2 .

2.2 Measurement Technique

2.2.1 Detectors

The first problem in measuring the spectral attenuation of optical fibers in the region from 600-1500 nm is finding a suitable detector (s). Table 1 lists information on a variety of detectors which could be used in this spectral range. The important parameter is the detectivity D which indicates the sensitivity and is inversely proportional to the root-mean-square voltage contributed by the noise. For some detectors the noise-equivalent power (NEP) (the optical signal equivalent to the internal detector noise) is given. The values D and NEP are related by:

$$D = \frac{\sqrt{A}}{NEP} \quad (1)$$

where A is the diode area. In Table 1 only one value of D or NEP is given although it has a spectral dependence determined by the quantum efficiency. For our measurements of spectral attenuation, two

* Some information taken from Laser Focus Buyers Guide 1976.

TABLE 1

TYPE	NEP ($\text{WHz}^{-1/2}$) or D ($\text{cm Hz}^{1/2} \text{W}^{-1}$) $D = \frac{\sqrt{\text{AREA}}}{\text{NEP}}$	$\lambda \mu\text{m}$	RESPONSIVITY a or v/w @ λ	$^{\circ}\text{k}$	AREA mm^2	MANUFACTURER	PRICE
Silicon	NEP = 2.7×10^{-13}	0.9	0.57 @ 0.9	300	20.3	Silicon Detector	\$ 20.00
	* 2×10^{-13}	1.06	0.5 @ 1.06	295	5	RCA Electro Optics	-
Germanium	NEP = 8×10^{-12}	1.4	0.87 @ 1.4	300	1	ROFIN	80.00
	D = 10^{11}	1.5	0.4 @ 1.5	295	1	Judson Infrared	70.00
	* NEP = 10^{-11}	1.5	0.6 @ 1.5	295	1	RCA	-
Lead Sulfide	D = 2×10^{10}	2.2	$4 \times 10^3 \text{ V}$	300	2.25	Infrared Ind.; East	37.50
	D = 5×10^{10}	2.1	$10^4 - 10^6 \text{ V}$	298	.06-100	Optoelectronics	-
Pyroelectric	D = 10^8	10	50V @ 10	-	4	Plessey Optoelectronics	118.00
	3×10^8	0.6	900V	-	.8-19	Molelectron	220.00
	* NEP = 1.07×10^{-9}		354V	-	1.0	Laser Precision Corp.	200.00

* TESTED OR USED AT BNR

detectors were chosen; first, a silicon detector for the range from 600-1050 nm with a NEP of approximately $2 \times 10^{-13} \text{ WHz}^{-\frac{1}{2}}$ at 900 nm and secondly, a RCA germanium PIN for the range from 1050-1400 nm with a NEP of approximately 10^{-11} at 1.5 μm . Fig. 4⁽²⁾ shows a graph of relative efficiency versus wavelength for both detectors.

A pyroelectric IR detector manufactured by Laser Precision Corp. with a NEP of $1.1 \times 10^{-9} \text{ WHz}^{-\frac{1}{2}}$ was tested because this detector shows a flat spectral responsivity extending well over the entire range of interest. However, as our light power levels were too low it was not satisfactory.

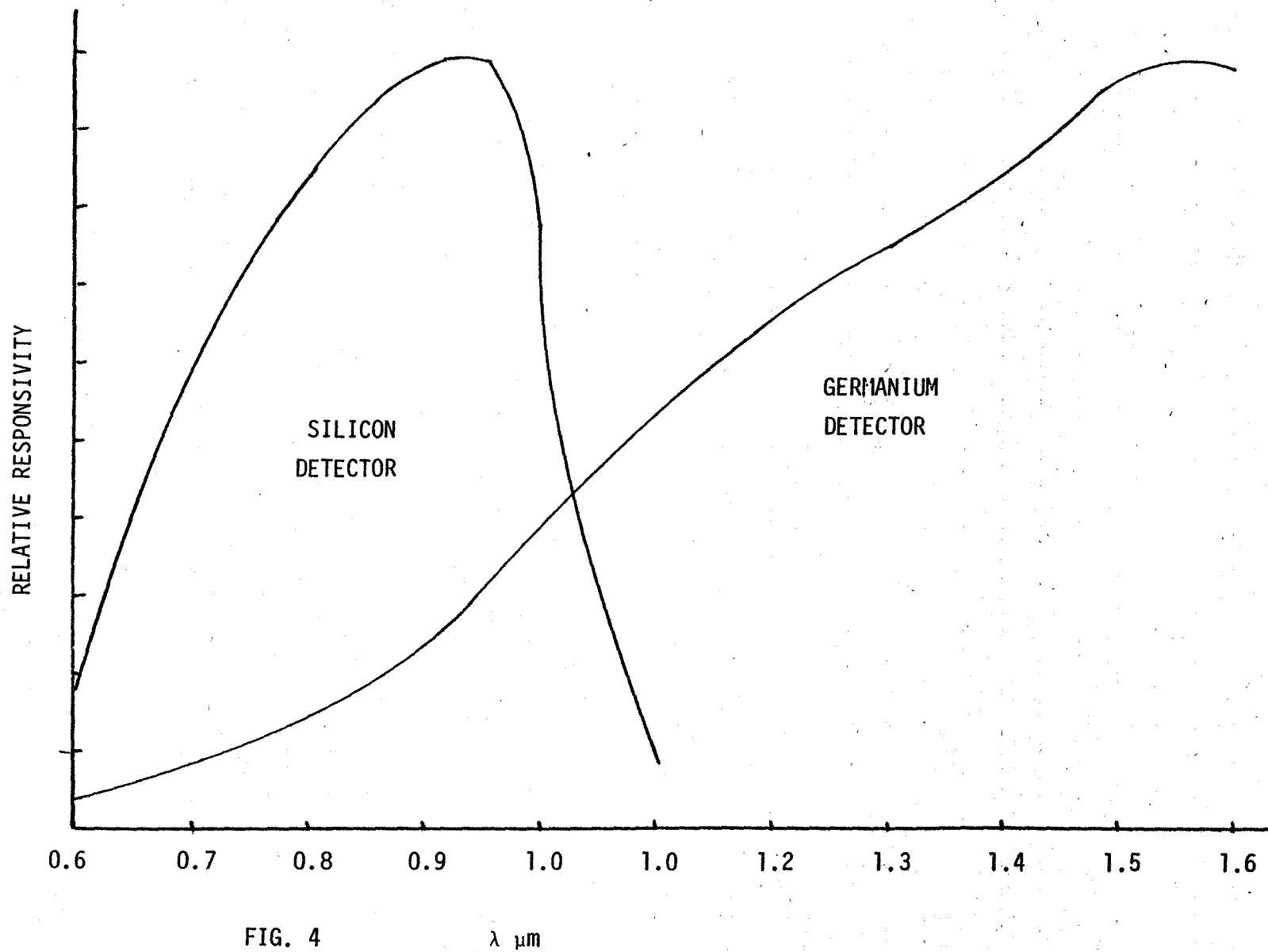


FIG. 4

Relative Response vs Wavelength for Silicon & Germanium Detectors

2.2.2 Direct Display of Optical Fiber Spectral Attenuations (3)

In a conventional technique, spectral attenuations have been calculated point by point from spectral light-output-power curves measured for the full length and the short length (typically 1 m) of sample fibers. Fig. 5 shows examples of the spectral light-output-power curves measured using a solar cell and a Ge-PIN diode for 600-1100 nm and 900-1500 nm regions, respectively. A few technical difficulties have been experienced in this method:

- (1) The measurement is sensitive to the optical and electronic alignments. Therefore, the measurement setup has to be extremely stable during the measurement.
- (2) The measurement and the following data processing are time consuming.
- (3) The final spectral attenuation curve has to be drawn by hand from the calculated points. Inaccuracies can easily be incurred because of any slight shift in the X axis during measurement.

Because of these technical difficulties, the spectral attenuation measurement has not been included in the routine characterization of optical fibers.

Using a new technique described below (developed during the work term) it is possible to display the spectral attenuations in dB/km directly on a X-Y recorder without using any sophisticated equipment such as a computer and a data acquisition system. A block diagram of the measurement setup is shown in Fig. 6.

In a conventional technique, the fiber attenuation ($A(\lambda)$) has been calculated using the following formula (2):

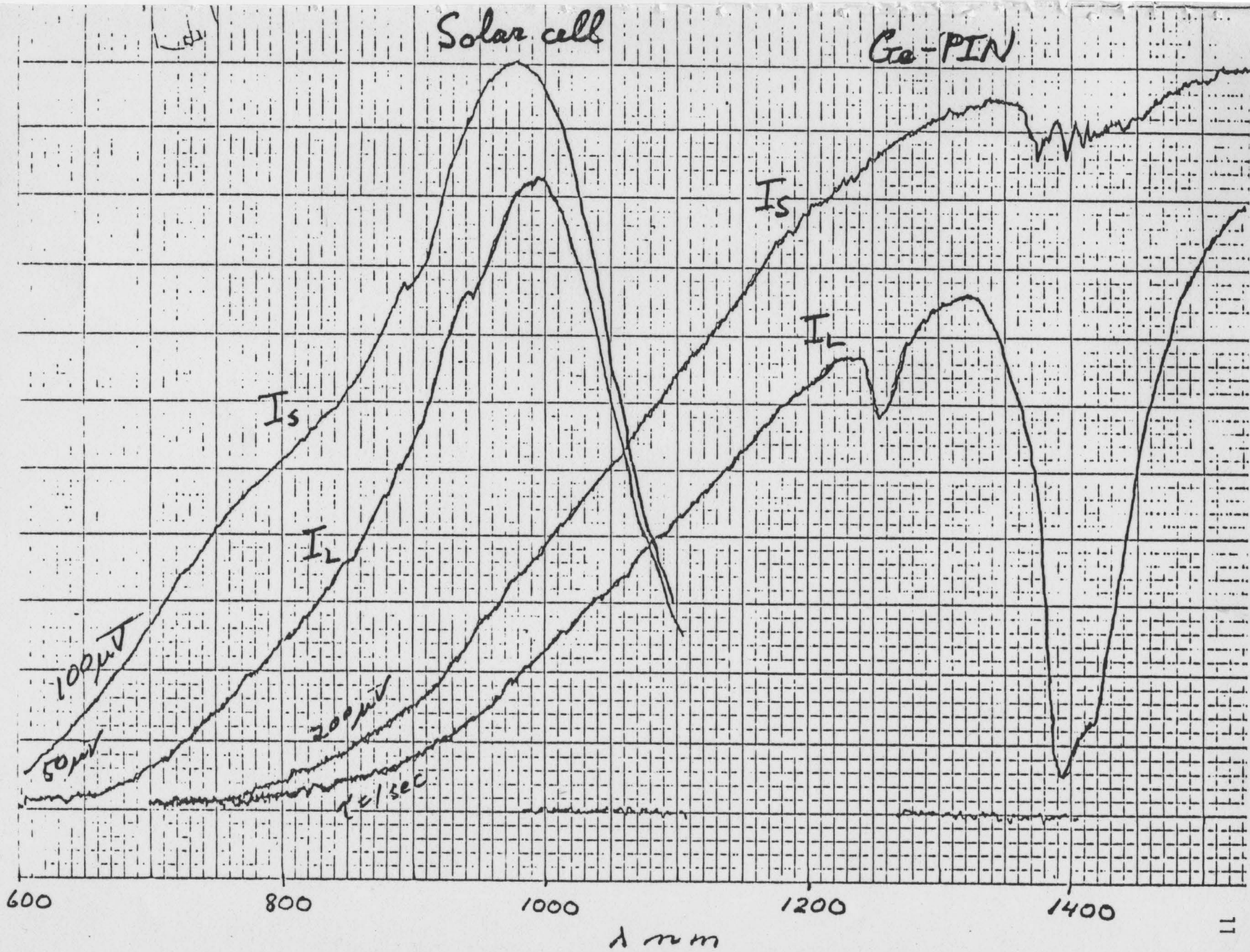


FIG. 5 CONVENTIONAL TECHNIQUE FOR MEASURING SPECTRAL ATTENUATION.
 Long and short fiber output curves are spectrally scanned for both detectors.

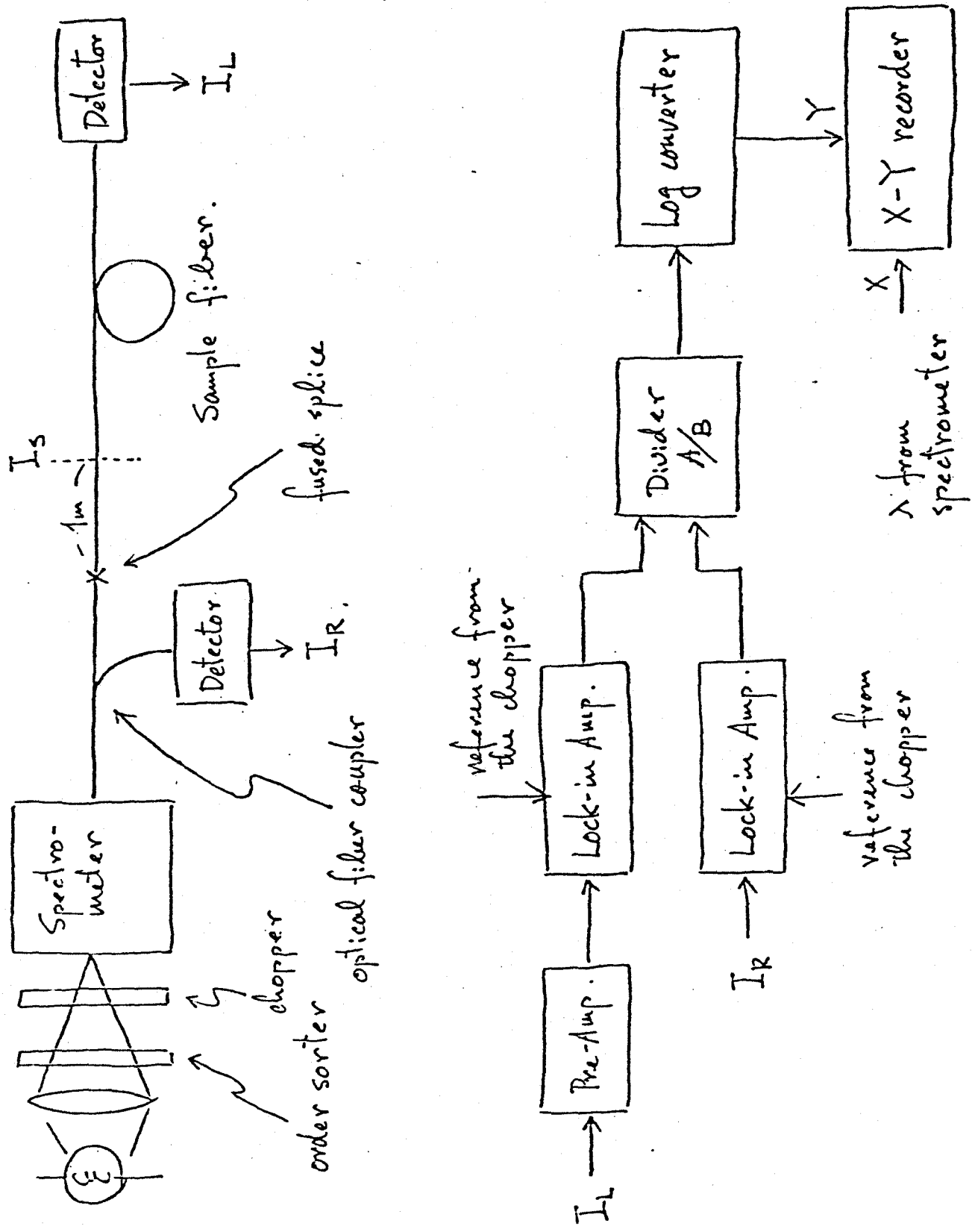


FIG. 6 NEW MEASUREMENT SETUP FOR SPECTRAL ATTENUATION

$$A(\lambda) = C_1 \cdot \log \frac{I_S(\lambda)}{I_L(\lambda)} \quad (2)$$

where I_L and I_S are the light-output-power measured sequentially for the full length and the short length of the sample fiber, and C_1 is $10/L$ (L is the fiber length in km to give the attenuation in dB/km). In the new technique, the monochromatic input light was divided into two channels using an optical fiber coupler. One channel was spliced to the sample fiber and the light output power ($I_L(\lambda)$) was monitored using the first detector. The light output power from the other channel was monitored using the second detector giving a reference signal ($I_R(\lambda)$).

Assuming

$$I_S(\lambda) = C_2 \cdot I_R(\lambda) \quad (3)$$

the attenuation of the fiber was displayed directly on the X-Y recorder as follows,

$$A(\lambda) = C_1 \left(\log C_2 + \log \frac{I_R(\lambda)}{I_L(\lambda)} \right) = C_4 + C_5 \cdot V(\lambda) \quad (4)$$

where C_1 , C_2 and C_5 are proportional constants and $V(\lambda)$ is the output voltage from the logarithm converter. Knowing the attenuation at the LED wavelength ($A(0.84 \mu\text{m})$) accurately, and simulating a higher attenuation by reducing the I_L - channel signal electronically, the base line (C_4) and the gain (C_5) are adjusted in such a way that the display of the $V(\lambda)$ on the X-Y recorder gives the fiber attenuation in dB/km directly.

One example of spectral attenuation curves measured by this technique is shown in Fig. 7. This particular fiber (No. 262 and 263 are spliced to give 2.3 km length) showed exceptionally high OH absorption peaks.

The accuracy of the assumption (3) was examined experimentally by displaying:

$$\log \frac{I_S(\lambda)}{I_R(\lambda)} = \log C_2 \quad (5)$$

on the X-Y recorder. The results are shown in Fig. 8 for the solar cells and the Ge-PIN diodes used in the present work. It is obvious from the figure that the assumption holds well in the wavelength range where the detectors have enough sensitivity. Residual experimental errors in this technique (from 0.2 to 0.5 dB/km depending upon the fiber length) are due to the mismatch of the two detectors. This error will be reduced by using one detector and modulating the two channels with different frequencies or by choosing two well matched detectors.

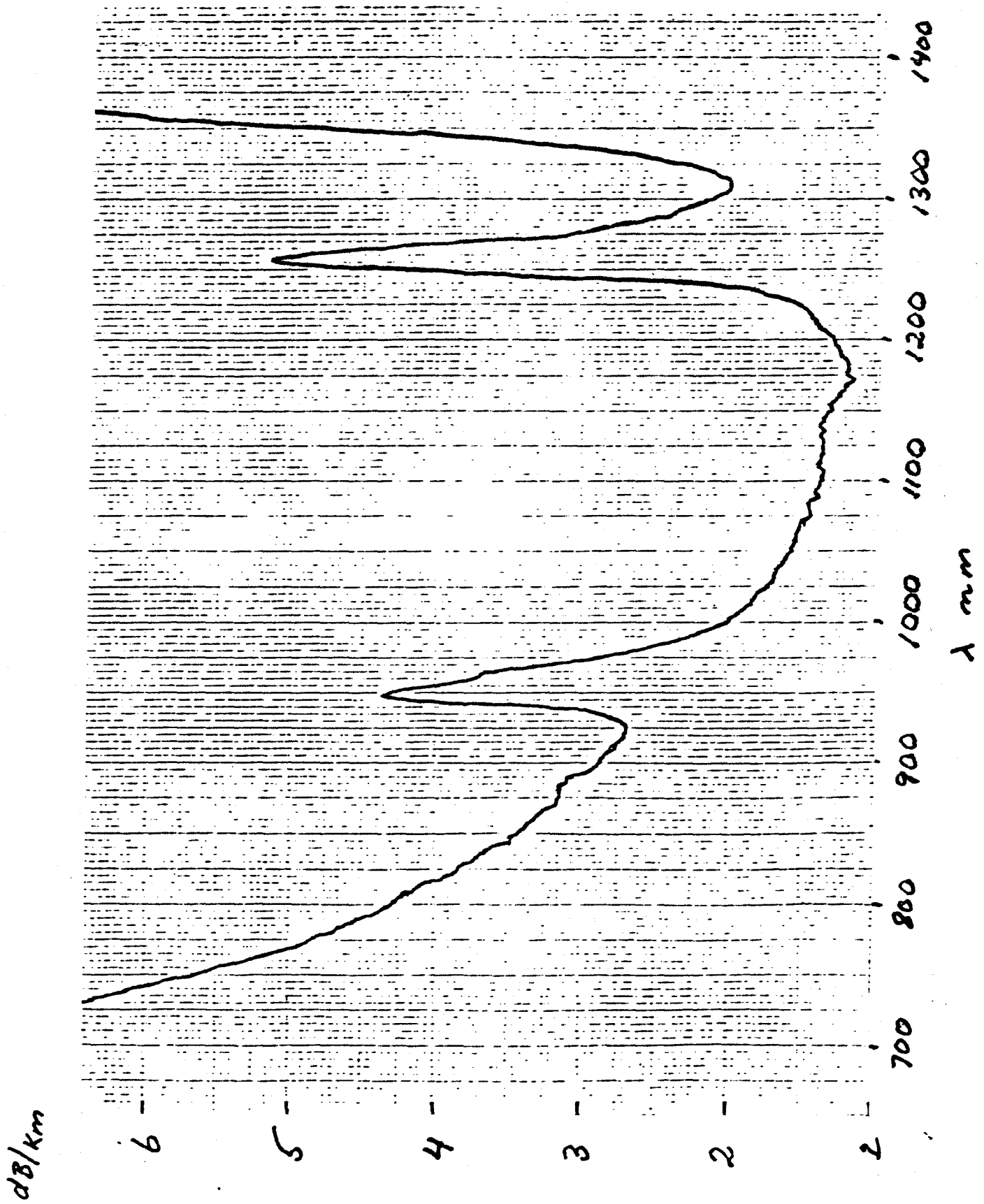
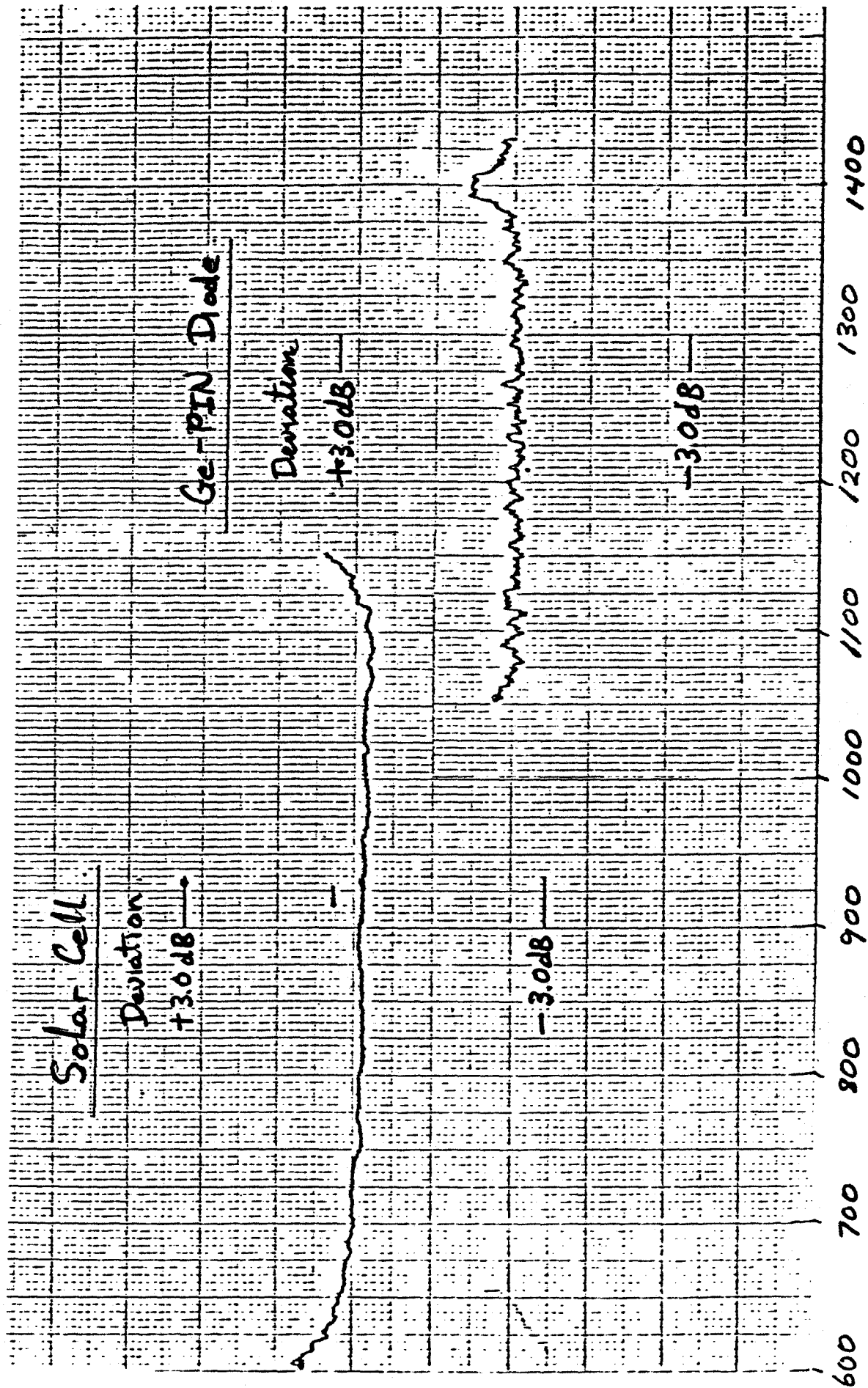


FIG. 7 SPECTRAL ATTENUATION CURVE FOR 2.3 KM FIBER SHOWING LARGE OH⁻ ABSORPTION PEAKS



λ nm

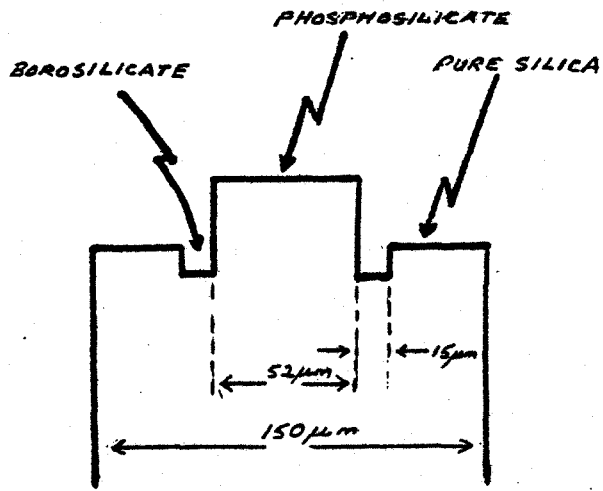
FIG. 8 GRAPH OF $\log \frac{I_S(\lambda)}{I_R(\lambda)}$

2.3 Examples of Spectral Attenuations

2.3.1 Phosphorus-Doped Silica-Core Fibers

Of all existing optical glasses, pure fused silica is known to have the lowest optical attenuation in the red and near infrared portion of the spectrum. The addition of P_2O_5 to silica results in an increased refractive index without a significant accompanying increase in the low-loss characteristic of pure silica. It has also been found that the material dispersion of phosphosilicate glass is no greater than that of fused silica, a property which germania doped silica does not exhibit.⁽⁴⁾ The lowest attenuation reported as of May 1976 was that of a very low OH content fiber consisting of a borosilicate cladding and a phosphosilicate core fabricated by the chemical vapour deposition process.⁽⁵⁾ It had a loss of 1.6 dB/km at 0.84 μm and 0.5 dB/km at 0.2 μm measured with a launching numerical aperture of 0.05. A similar fiber was made at BNR to get an idea of the lowest possible attenuation achievable in the preform fabrication process at that time. The starting materials were $POCl_3$ (Baker Chemicals) BBr_3 (Apache Chemicals) and $SiCl_4$ (Air Products) used without any purification. It was a step index fiber but with a "w" shaped profile. The core diameter was typically 52 μm (see Fig. 9) and the cladding thickness of the boron doped silica layer was 15 μm . The fiber was pulled to a diameter of 150 μm and coated with silicone. Using our standard measurement technique, but limiting the launching NA to 0.05, the attenuation of this fiber was measured as 2.1 dB/km at

* Please refer to section on attenuation vs launching N.A., p. 34.



"W" SHAPED INDEX PROFILE FIBER #288

FIG. 10

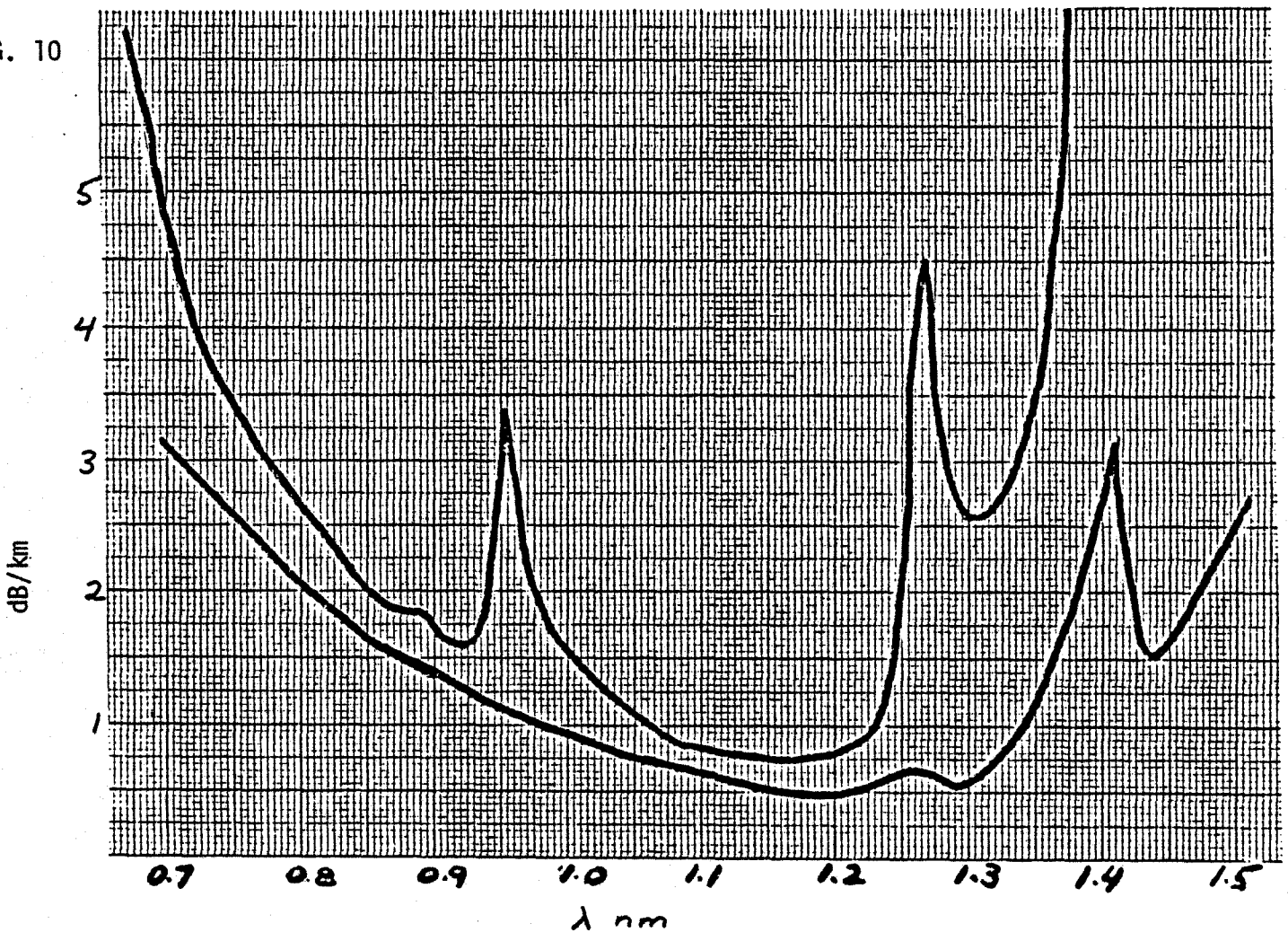


FIG. 10 SPECTRAL ATTENUATION OF P-DOPED SILICA CORE B-DOPED CLADDING FIBER #288 1065 n LAUNCHING NA = 0.05

0.84 μm . The spectral attenuation curves for both BNR's fiber and the referenced lowest loss fiber is shown in Figure 10. ⁽⁶⁾ The residual 0.5 dB/km extra loss over that reported by Horiguchi may be attributed to either impurities in the starting chemicals, a winding effect, diameter variations, or an effect of the coating. Also, since no attempt had been made to remove the impurities in the BNR fiber, the OH peaks at 0.95 and 1.23 and 1.4 μm are very large. In the Horiguchi fiber all the halides were refined by distillation in advance of deposition and the SiCl_4 was purified to be free from trichlorosilane and other compounds which contain hydrogen. In this manner the OH content in the glass was reduced to several tens of parts in 10^9 .

2.3.2 Silicone-Cladded Silica-Core Fibers

Plastic-clad silica (PCS) fiber has the advantages of being easily fabricated, having a large numerical aperture and large step index core. This makes it well suited for the low capacity, short to medium haul transmission of the incoherent light from light emitting diodes. Among the plastics with indices lower than that of pure fused silica ($n = 1.458$) which have been tried as cladding materials are Teflon FEP100 (fluorinated ethylene-propylene $n = 1.338$) and hexafluoropropylene and vinyl fluoride ($n = 1.415$). However, silicone resin ($n = 1.405$) has a much lower loss than any of the above polymers and has yielded sub 3 dB/km fibers at 0.84 μm . Silicone resin itself has an attenuation similar to that of ordinary optical glass; at 0.84 μm its loss is 3000 dB/km. The loss of the cladding material is important as it actually induces an additional loss to the light in the core. The relationship is given by the equation: ⁽⁷⁾

$$\alpha = \alpha_{\text{CORE}} + \frac{\alpha_{\text{CLAD}} - \alpha_{\text{CORE}}}{2akNA} \quad (6)$$

where α is the attenuation of the fiber
 α_{CORE} is the attenuation of the CORE
 α_{CLAD} is the attenuation of the CLADDING
 a is the core radius

$$k = \frac{2\pi}{\lambda}$$

Thus in a PCS fiber, since α_{CLAD} is much greater than α_{CORE} , the additional loss is nearly proportional to the cladding loss.

Fig. 11 and 12 show spectral attenuation curves for silicone cladded silica core fibers made at BNR by using Shin-etsu silicone KE-103 and synthetic vitreous fused silica rods:

(A) Silanox WF from Komatsu Electronics Metal Co.

(B) Suprasil 2 from Heraeus-Amersil Co.

The WF fiber has a much lower water content, however, it is also more expensive. Absorption bands at 0.91, 1.1, 1.2 μm are due to the silicone cladding. The lowest attenuation in the Silanox fiber is 2.6 dB/km at 0.84 μm . Towards the longer wavelengths there are two narrow, transparent windows of 4 and 3 dB/km at 0.99 and 1.06 μm respectively. The low attenuation value of 2.6 dB/km at 0.84 was measured with an LED source attached to a 500 m pigtail of similar fiber. This corresponds to a launching numerical aperture (100% points) of approximately 0.24 which is nearly the same as that of the steady state condition. Both the Silanox and the Suprasil fibers have a core diameter of 120 μm with a total diameter of 350 μm .

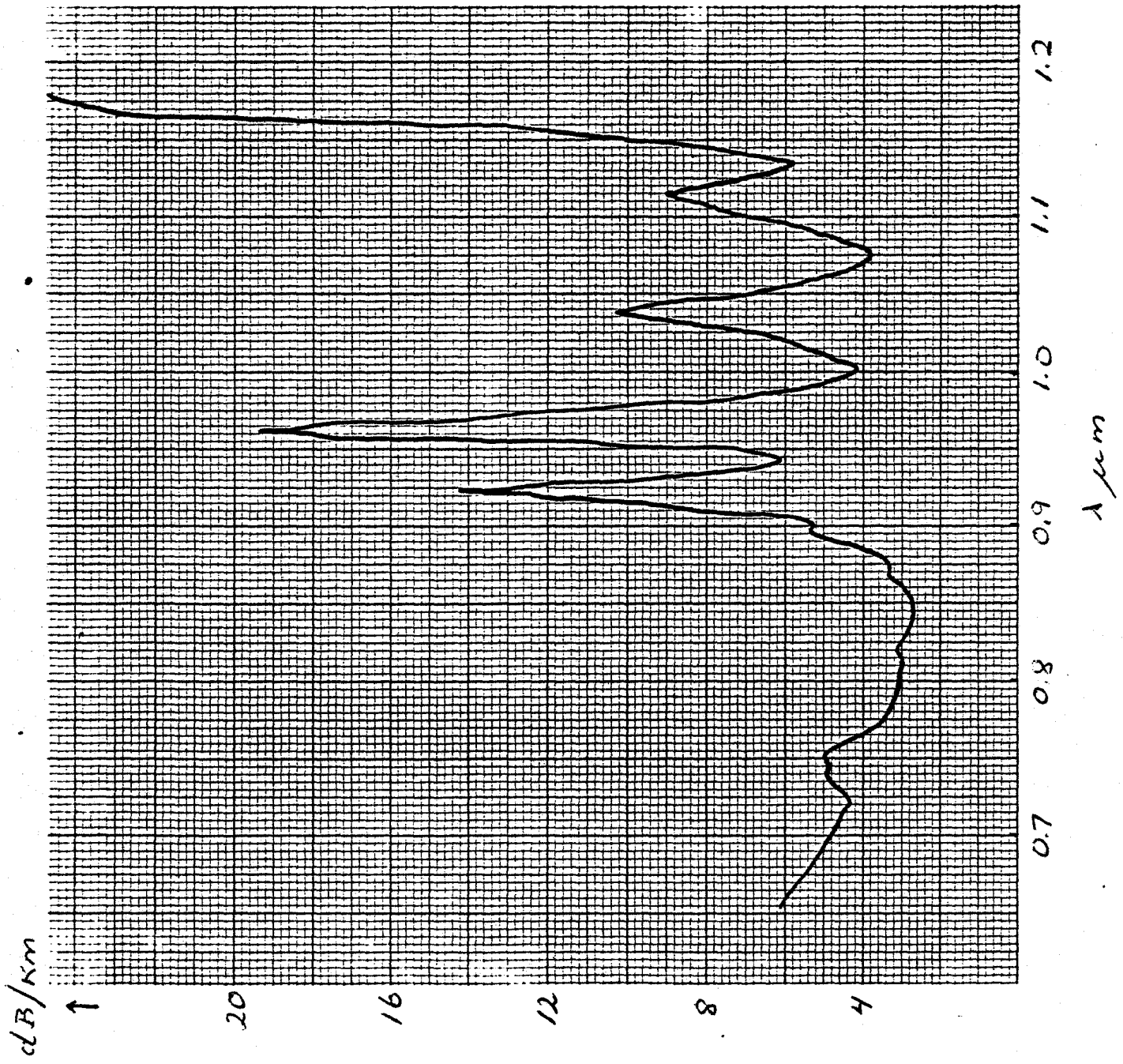


FIG. 11 SPECTRAL ATTENUATION OF SILANOX-WF WITH SHIN-ETSU 103 SILICONE CLADDING

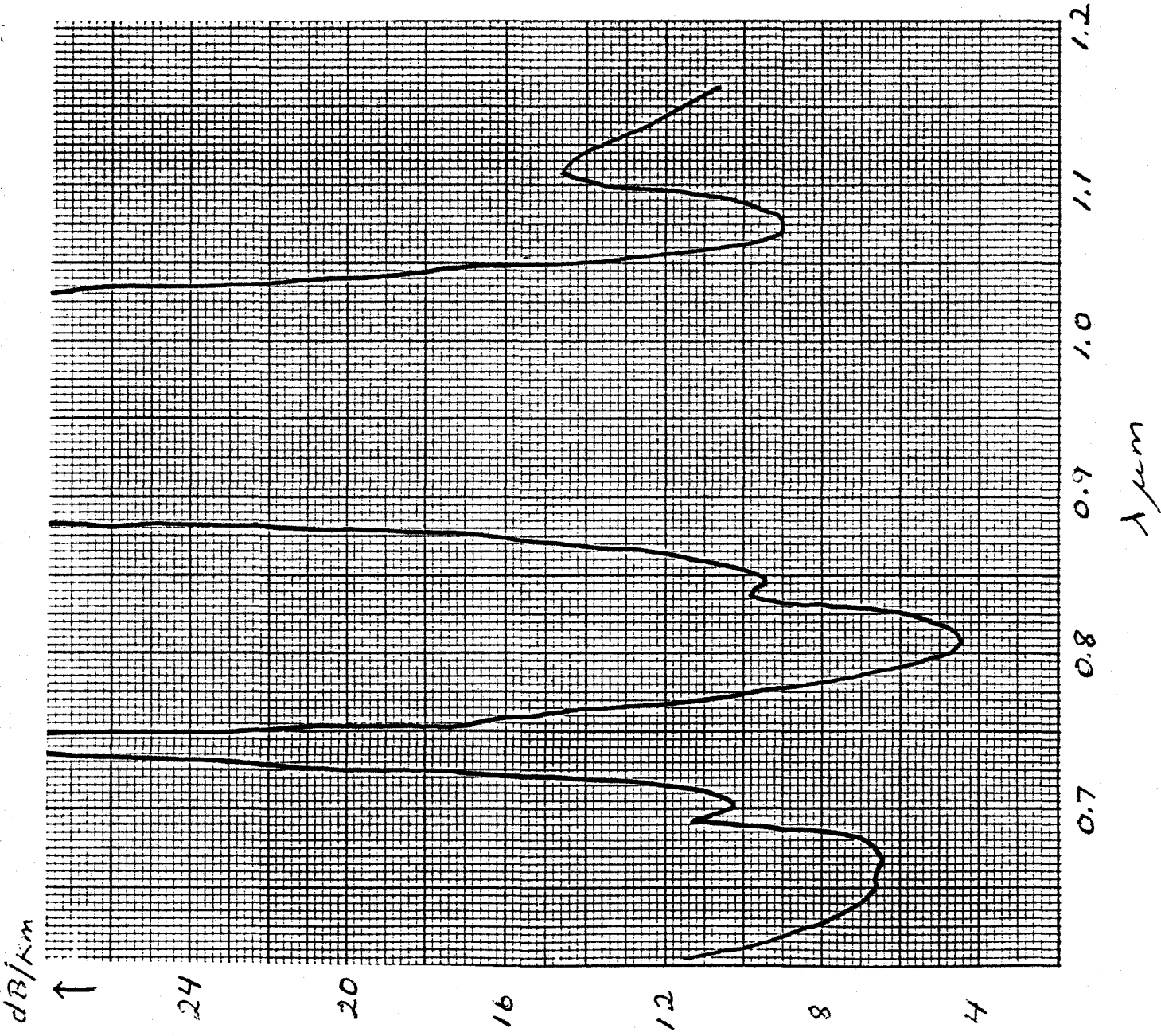


FIG. 12 SPECTRAL ATTENUATION OF SUPRASIL-2 WITH SHIN-ETSU 103 SILICONE CLADDING

CHAPTER 3

ATTENUATION CONSIDERATIONS

3.1 Optical Power vs. Length

3.1.1 General Description

In general the optical power at a distance Z from an input is given by:

$$P(Z) = P(0) \text{ EXP. } \left[- \int_0^Z \alpha(Z) dZ \right] \quad (7)$$

(obtained from the rate equation for loss $\frac{dI}{dZ} = -\alpha(Z)I$)
where $\alpha(Z)$ is the loss coefficient and $P(0)$ is the power in the fiber at position $Z = 0$. When the steady state distribution has been achieved, $\alpha(Z)$ is constant and only then is it valid to quote the attenuation in dB/km. Mode coupling eventually establishes the steady state condition by statistically compensating the differential loss between the higher order modes which penetrate more into the lossier cladding, and the lower order modes of the fiber. It can be determined experimentally whether or not the steady state distribution has been obtained. One necessary condition is that a plot of the log of the output power versus length becomes linear. Another necessary condition is that the far-field radiation pattern becomes constant. Figures 13 and 14 are graphs of both the output power and the log of the output power versus fiber length for a 350 meter section of a 75 μm core graded index fiber. The launch condition was a direct butt up to a BNR LED (centered at 840 nm) which had an approximately Lambertian output. As determined from Figure 14, steady state has been achieved after only 50 m (some

FIG. 13

OUTPUT POWER VS LENGTH (FIBER #228)

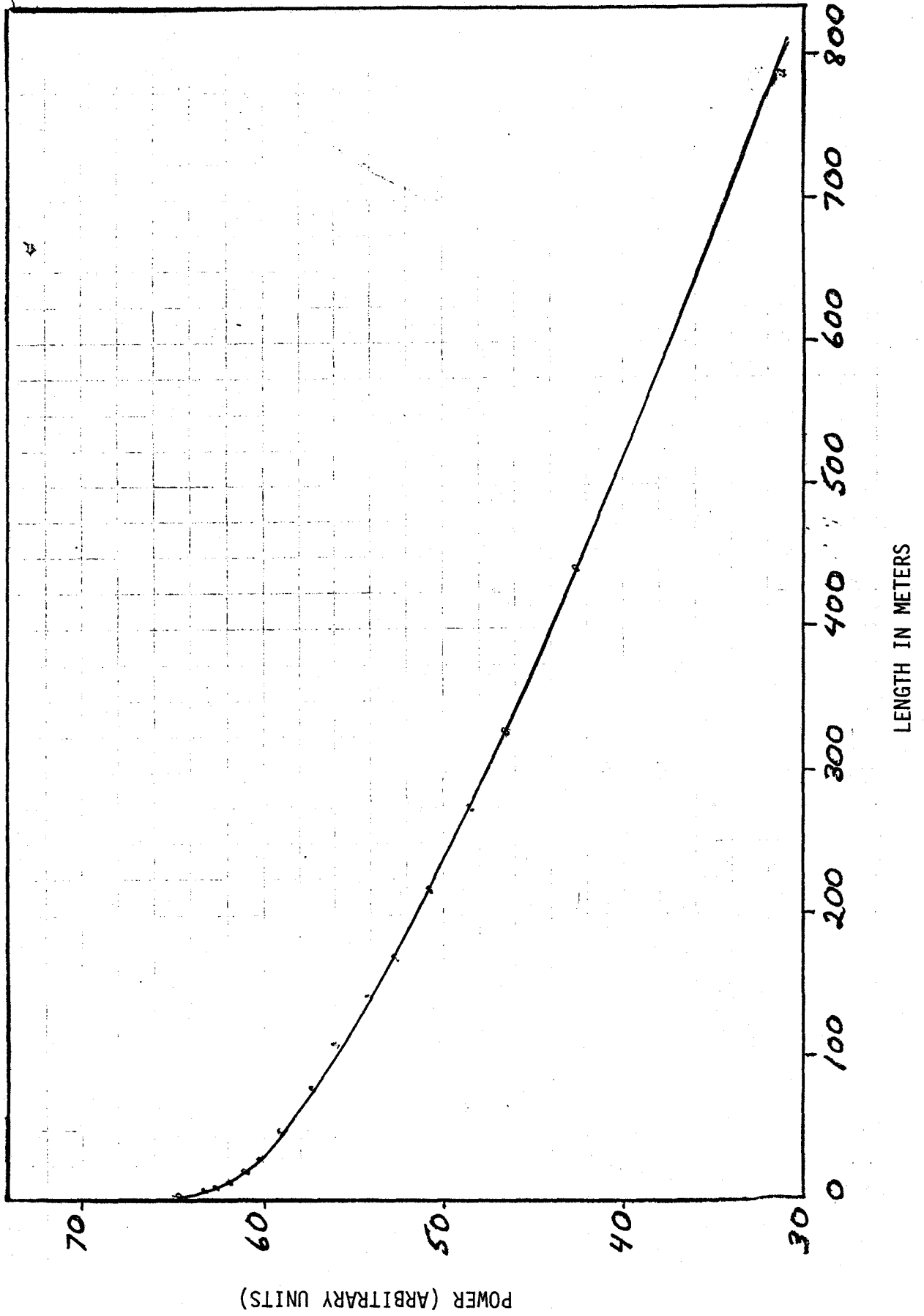
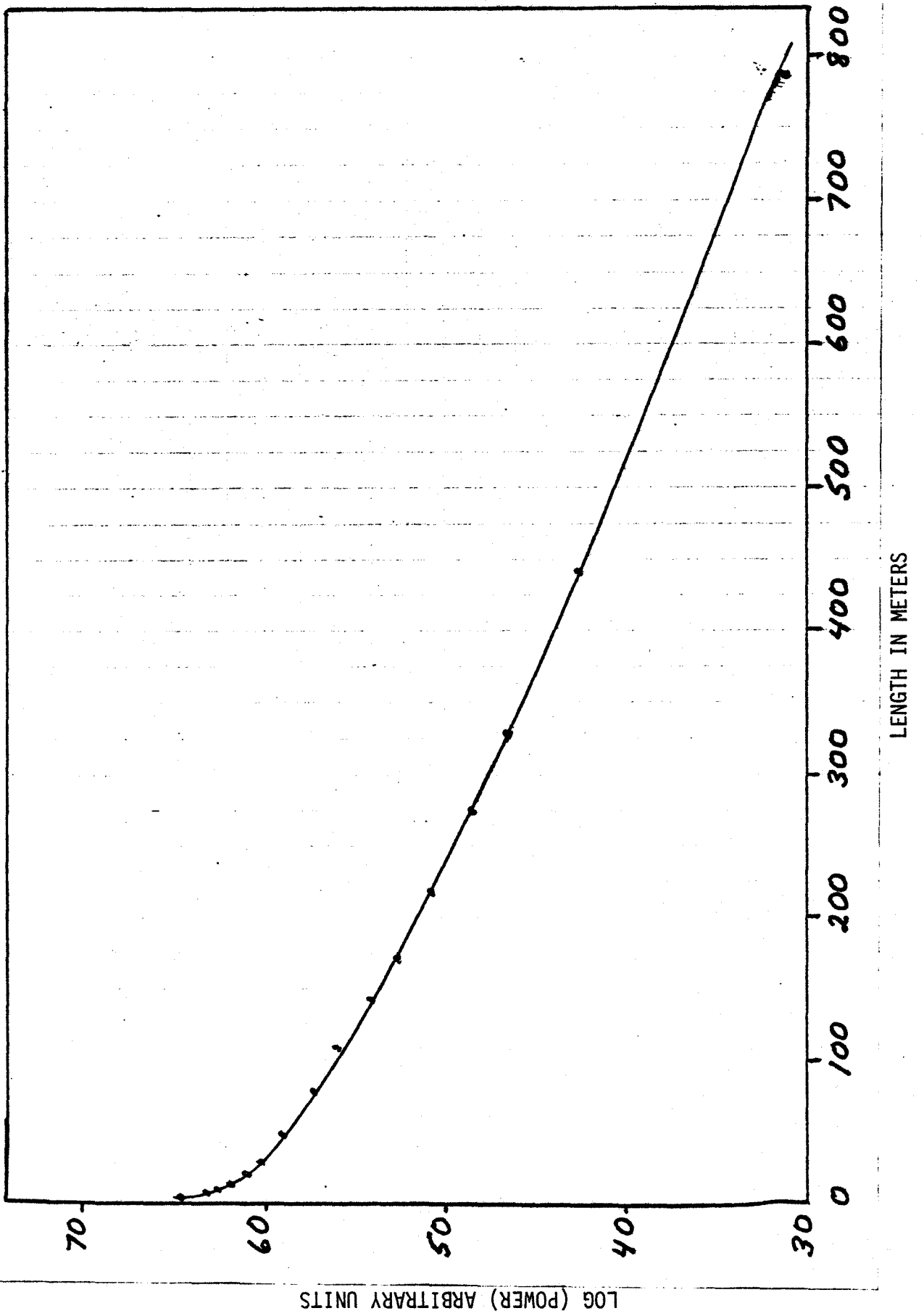


FIG. 14 LOG (OUTPUT POWER) VS FIBER LENGTH (FIBER #228)



fibers have not reached a steady state after several hundred meters). At this point the numerical aperture of the fiber dropped by 0.03 from a short length (1 meter) N.A. of 0.22.

In the characterization of optical fiber at BNR, the steady state attenuation is now being measured^{*} by fusion splicing the fiber to be measured, to a "pigtail" fiber, which has an LED input and is longer than the steady state length. The output from the far end of the fiber being characterized is then compared with the input obtained by breaking the fiber about 1 meter downstream from the splice. A "pigtail" fiber is made up (i.e. an LED is permanently attached) for every type of fiber being produced. Each should have a core size and N.A. at the bottom end of the specifications for the fibers it is used to characterize.

3.1.2 Silicone-Coated Fibers

As of the summer of 1977, silicone has been used as the protective coating for all fibers made at BNR. Previously, both nylon and "hytrel"^{*} were used but were both found to cause excess temperature-dependent attenuation.^{*} The use of silicone solved this problem but at the same time added some interesting effects. Silicone is one of the few substances which has a refractive index lower than that of pure silica. Therefore, in a silicone-coated fiber there is actually another waveguide formed...that is between the cladding glass and the silicone cladding (light captured by this waveguide does, however, still pass

* As a result of the author's work on power vs. length measurements and on fusion splicing.

* A copolyester elastomer from Dupont.

* Please refer to section on attenuation vs temperature, p.40 .

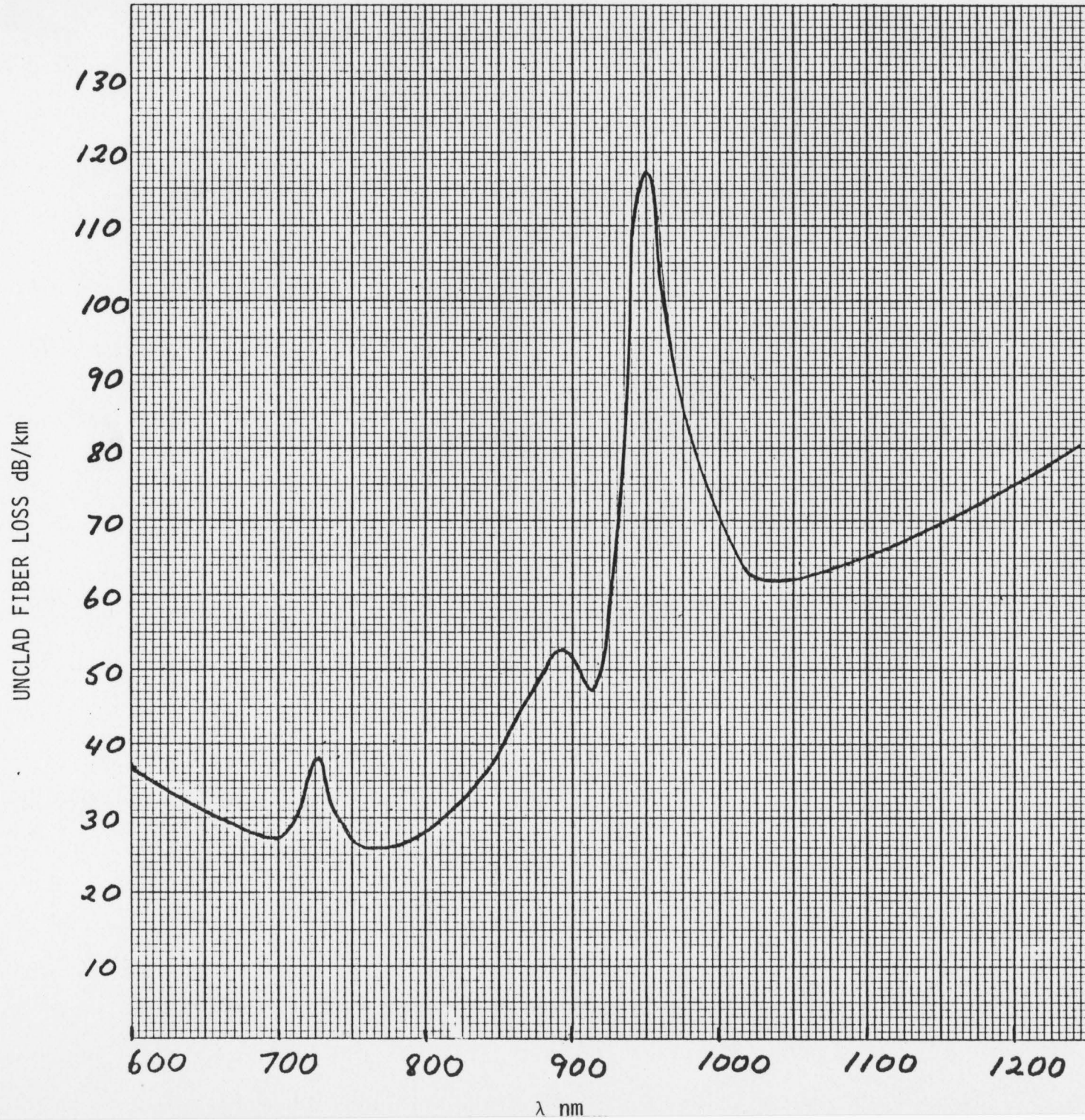
through the fiber core). The numerical aperture (short length) of this waveguide is 0.41 ($=\sqrt{(1.46)^2 - (1.40)^2}$).

In the CVD process used at BNR, the cladding is formed from T08 (WG grade) quartz tubes obtained from Hereaus Amersil (New Jersey distributor). These tubes have a spectral loss as shown in Fig. 15. (8)
 With an LED centered at 840 nm the attenuation is approximately 20 dB/km. This was measured directly by a technique illustrated in Fig. 16. Light was inserted into the cladding by twisting a PCS fiber (attached to the LED) around a bared section of the graded index fiber. With about 10 twists a transfer of up to 1/3 of the light from the PCS fiber can be achieved. The attenuation in the cladding was then obtained by comparing the amount of cladding light after a 200 m length to the amount one meter from the twisted section.

Fig. 17 shows a log plot of POWER versus FIBER LENGTH for a graded index fiber both with and without the cladding light stripped out. The source was a BNR LED at 840 nm butted directly to the fiber (with no stripping). The particular fiber (NT44, 144 μm O.D., 80 μm CORE, 0.23 N.A.) used was chosen because it had a typical loss plus the fact that the core and cladding diameter stayed constant from the top to the bottom end of the reel. A gradual taper would cause undesired effects such as increased transfer from the core to the cladding. Note that, from the graph, there is a factor of over six times as much light collected by the cladding than by the core at the source. This is due to both the difference in the N.A. (0.41 for the cladding-silicone interface, 0.22 for the core) and because the cladding-silicone waveguide is effectively a step index waveguide

FIG. 15

SPECTRAL LOSS OF UNCLAD FIBER MADE FROM COMMERCIAL-GRADE T08



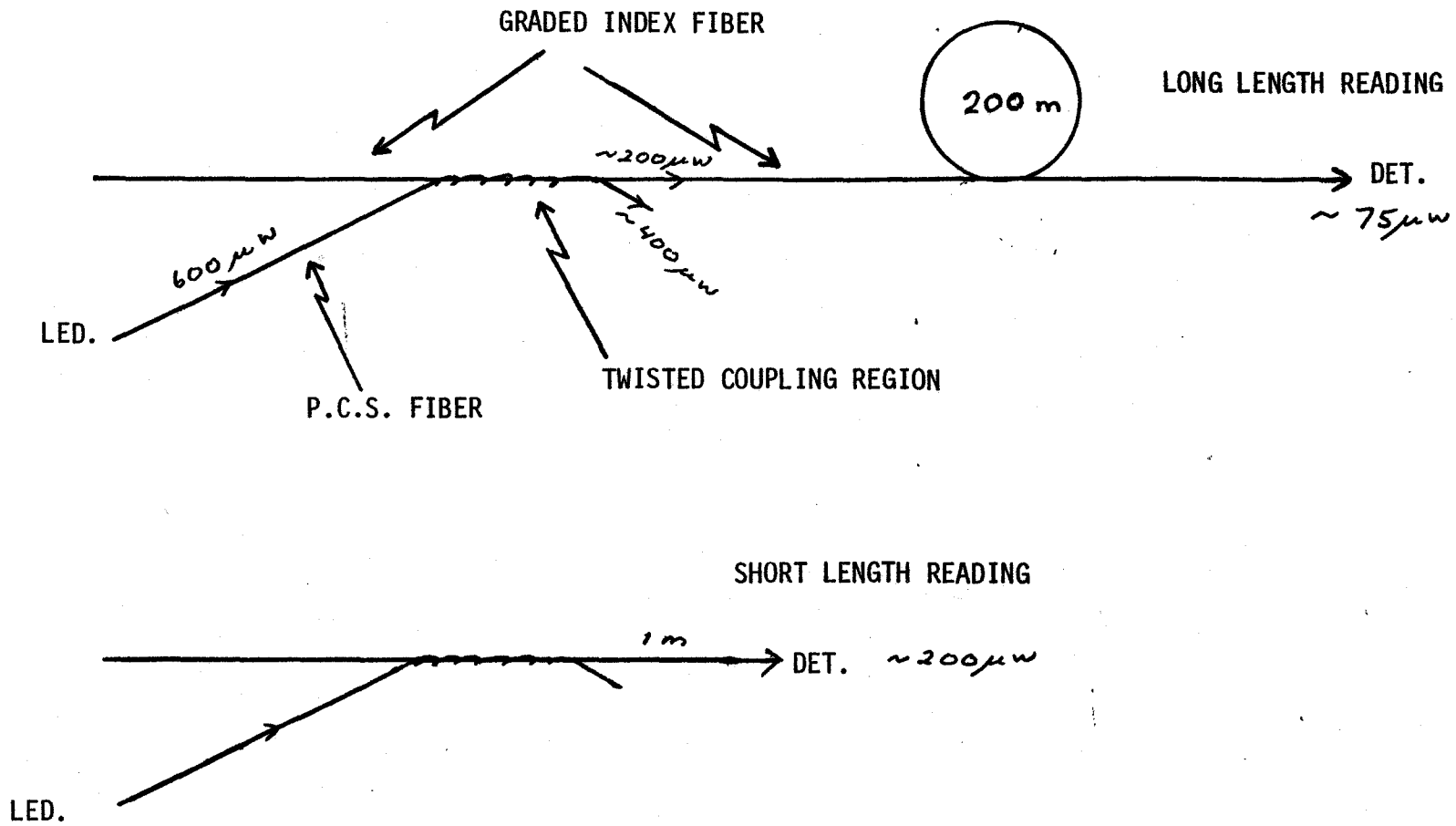
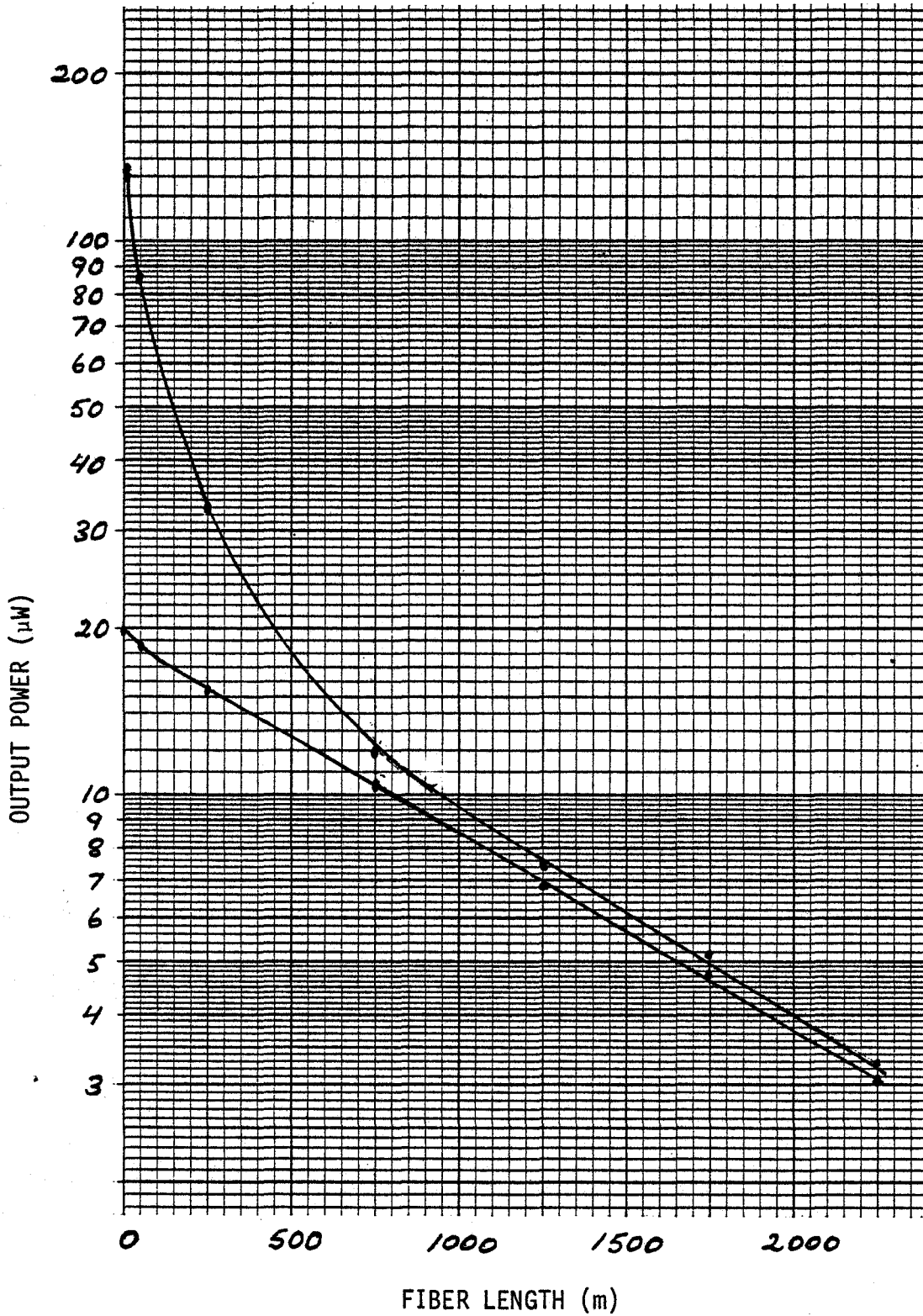


FIG. 17

POWER VS LENGTH
SILICONE COATED FIBER (YORKVILLE) NT44
(1) UNSTRIPPED AT DETECTOR
(2) STRIPPED AT DETECTOR



- READING MADE USING LED 428/46 AT 20 MA
- FIBER NT44 GRADED INDEX, 144 µm O.D., 80 µm CORE, 0.23 NA

(similar to a PCS fiber). The collection of light at the LED is illustrated in Fig. 18.

Even though there is a factor of 6 difference between cladding and core light near the source, the cladding light attenuates at about 20 dB/km while the core light attenuation is only slightly greater than 3 dB/km. Table 2 below shows the calculated relative power levels of core and cladding light after a distance of 1 and 2 km:

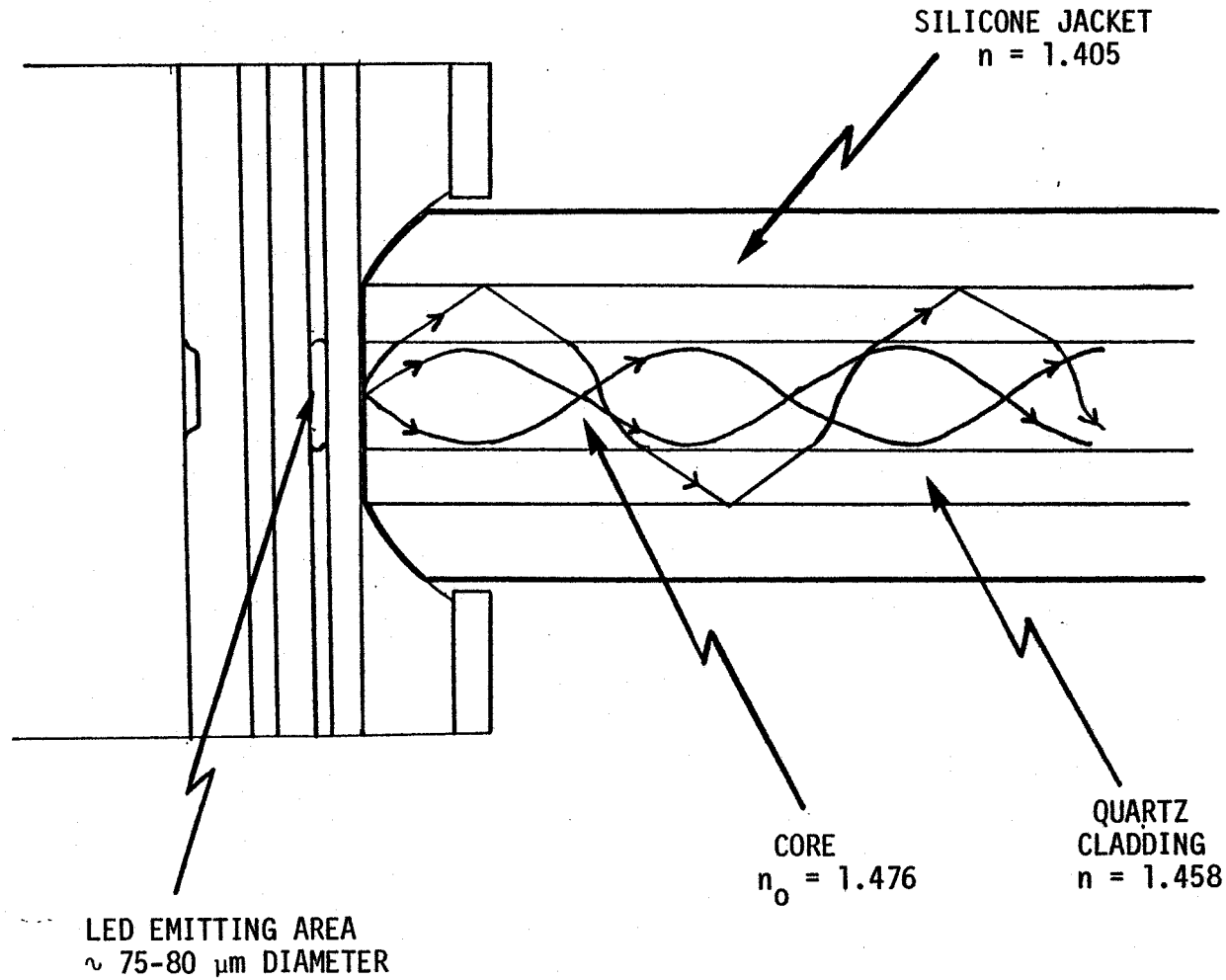
TABLE 2
POWER LEVELS (RELATIVE UNITS)

	INPUT	1 km	2 km
CORE	1	0.5	0.25
CLADDING	6	0.06	0.0006
(% of CORE LIGHT)	600%	12%	0.24%

The cladding light from the source is thus down to a mere $\frac{1}{4}\%$ of the core light after 2 km. A look at the graph of Fig. 17, however, shows that there is about 7% of cladding light. The difference is caused because some of the light lost from the core over the entire length of fiber is actually retained at the cladding-silicone interface. A calculation of the relative amount of cladding to core light (given by γ) versus fiber length is given in Appendix A. The results of this calculation show that after $1\frac{1}{2}$ to 2 km γ is effectively constant and is given by:

FIG. 18

LED LIGHT CAPTURED BY CORE AND CLADDING
OF A SILICONE COATED GRADED INDEX FIBER



$$\gamma = \frac{\text{CLADDING LIGHT}}{\text{CORE LIGHT}} = \frac{\beta^1}{k_2 - k_1} \quad (8)$$

where β^1 = light lost from core to cladding in dB/km

k_1 = attenuation in core in dB/km

k_2 = attenuation in cladding in dB/km

For the fiber of Fig. 17, β^1 is found to be approximately 0.7 dB/km.

This theory does not include the effects of micro and macro bends on the fiber which would further increase β^1 and the cladding to core ratio.

There is one fact that the analysis in Appendix A does not take into account. Not only is there transfer from the core to the cladding but there is also transfer in the reverse direction (it is not, however, as significant). This can be demonstrated by monitoring the output from, say, a 100 m length of fiber. The signal will drop by stripping the cladding light at the detector...yet it can also be made to drop even further (up to $\sim 3\%$) by stripping near the source. This effect should be taken into account when measuring splice or connector losses. It is generally advantageous to strip the cladding light in as many locations as possible.

The cladding waveguide of a silicone coated fiber could be used to an advantage in certain fiber systems. For example, in a high security link it can be used as a monitor to protect against tapping of the core light. It could also be utilized to return (or add in the same direction) a voice channel (or other low bandwidth information) to a main video link without causing extra loss. The cladding signal could

be inserted by using a twisted tap coupler as is illustrated in Fig. 19 (a). Fig. 19 (b) illustrates that up to 1/3 of the light inputted at A can be transferred to the cladding of the main trunk fiber. Although 2/3 is lost, it must be remembered that, say for example in Fig. 17, six times as much light can be inputted at A into the PCS fiber (or graded fiber used as a PCS fiber) than into the core of the main fiber. Some fibers made by BNR can collect 30 times more light in the cladding than in the core. * The light which is transferred to the cladding of the main trunk fiber normally has 20 dB/km loss for an LED at 840 nm when a T08 (Waveguide Grade) tube is used to make the preform. It is possible, however, to use "Silanox WF" or "Suprasil 2" fused silica tubes (normally bought in rod form to use as the core for PCS fibers) as a preform. This, together with a good quality silicone (Shin Estu KE103), can reduce the cladding loss to less than 3 dB/km at 840 nm (the spectral loss of the cladding would be as shown in Figures 11 and 12). The number of applications using the cladding as a waveguide would be greatly increased. The disadvantages, however, should also be given. They are (a) cost and (b) the fiber would have to be handled as a PCS fiber, i.e. extra care would be needed at splice joints so that cladding light is not removed.

3.2 Launch Conditions

3.2.1 Attenuation vs Launching Numerical Aperture

Specifying the launch conditions is very important when

* Please refer to section on Coupled Power from an LED, P.41 .

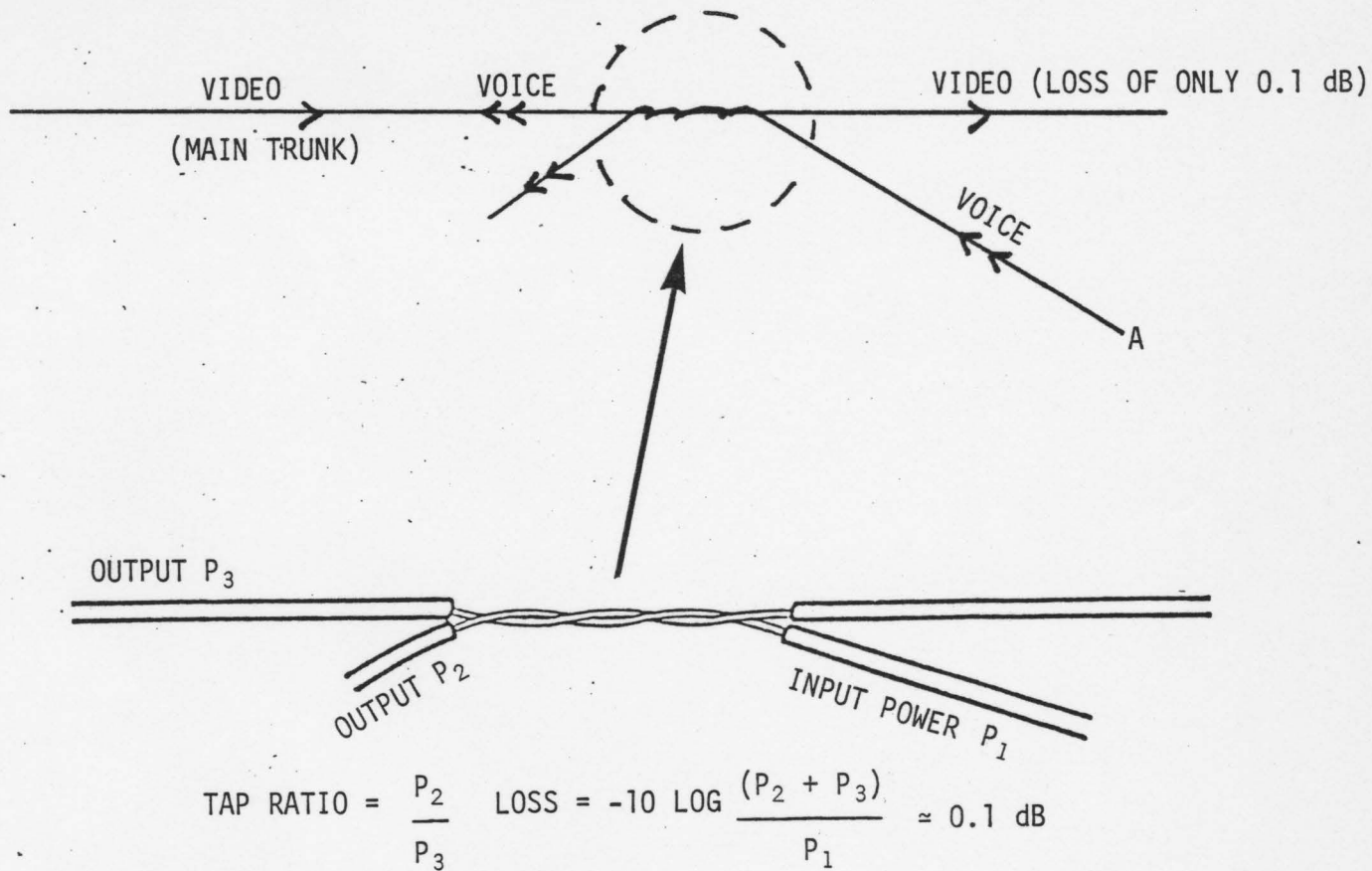
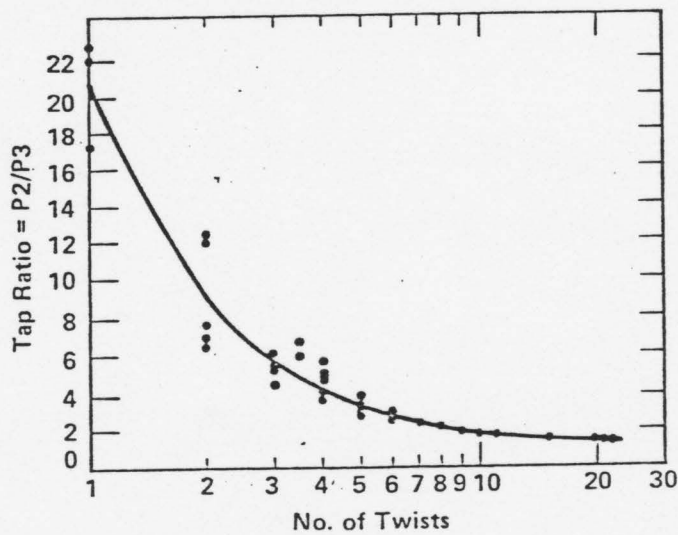


FIG. 19 (b) ACHIEVABLE COUPLING RATIO'S
 (BEST COUPLING TO OUTPUT P₃ IS APPROX. 1/3 P₁)



Tap Ratio vs. No. of Twists

reporting results of attenuation measurements. Fig. 20 shows the effect on fiber attenuation of varying the launching numerical aperture. The step index fiber had a 52 μm phosphorus-doped core and a boron-doped cladding with an N.A. of 0.18. The graded index fiber was Ge doped, had a 0.22 NA and a core and O.D. size of 85 μm and 150 μm respectively. In the experimental setup (shown in Fig. 21 (a)) it was required to restrict the spot size of the illuminating system to smaller than the core size. The fiber end was illuminated with a 20 μm diameter spot in order to minimize leaky mode excitation. It can be noticed that the attenuation remains constant when the launched N.A. exceeds the acceptance N.A. of the fiber. At the low end, the step index fiber reaches an attenuation of slightly less than 2.1 dB/km (a drop of 0.9 dB from the full N.A. excitation attenuation). The lowest value reported as of May 1976 was 1.6 dB/km with a launching N.A. of 0.05^{*}. The graded index fiber shows quite a different N.A. dependent attenuation. This is due to the higher germanium doping which causes a trade-off between the trend of lower attenuation with lower launching N.A. (as with the step index fiber) and the trend of increased attenuation towards the center of the fiber.

It is also possible to measure the modal dependence of attenuation. This measurement was not performed but the experimental setup which would be used is shown in Fig. 21 (b) and 21 (c). In a step index fiber each mode group can be selectively excited by illuminating the input fiber end with a plane wave at an angle to the fiber axis. There is a simple

* Horiguchi, p.311.

FIG. 20

ATTENUATION VS LAUNCHING N.A.

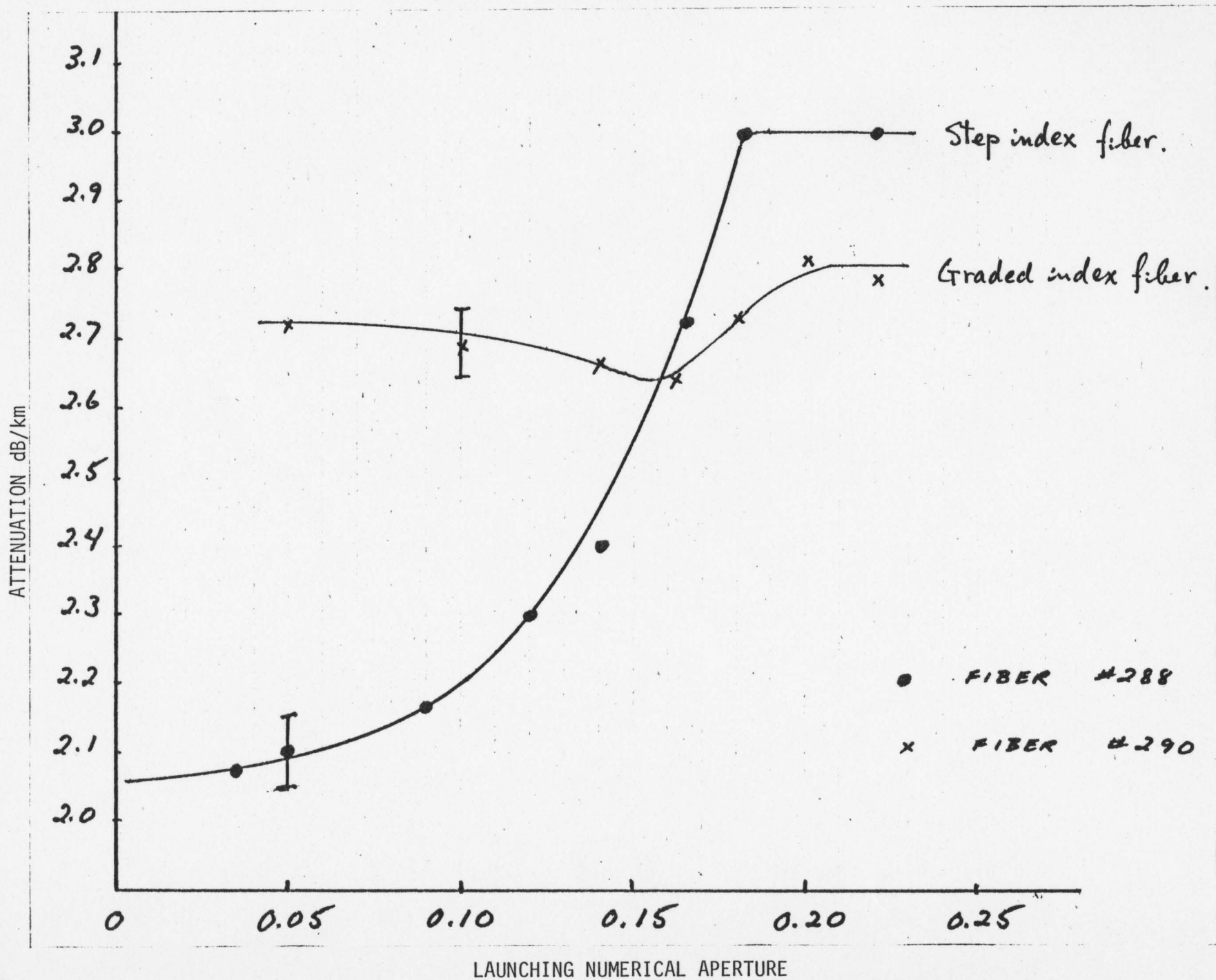


FIG. 21 (a) ATTENUATION VS LAUNCHING N.A. SETUP USED FOR FIG. 20

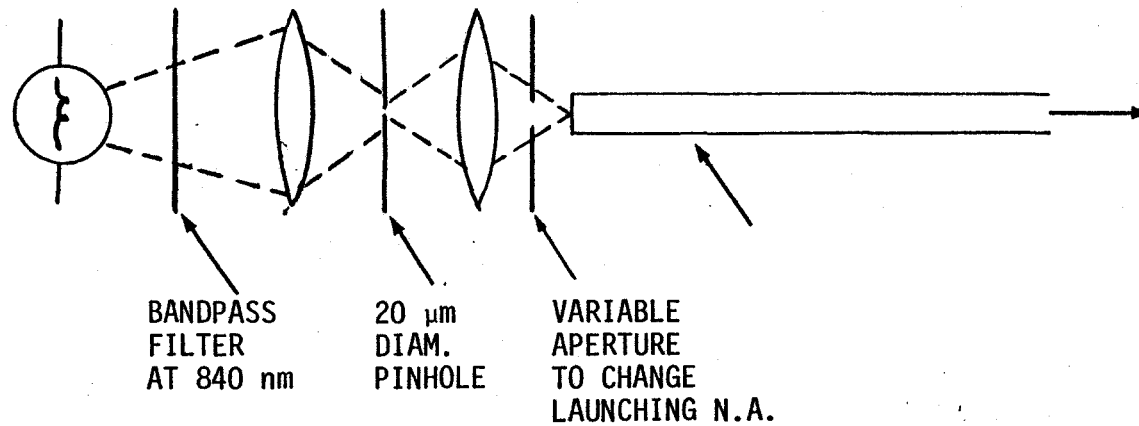


FIG. 21 (b) MODAL DEPENDENCE OF ATTENUATION FOR STEP INDEX FIBER

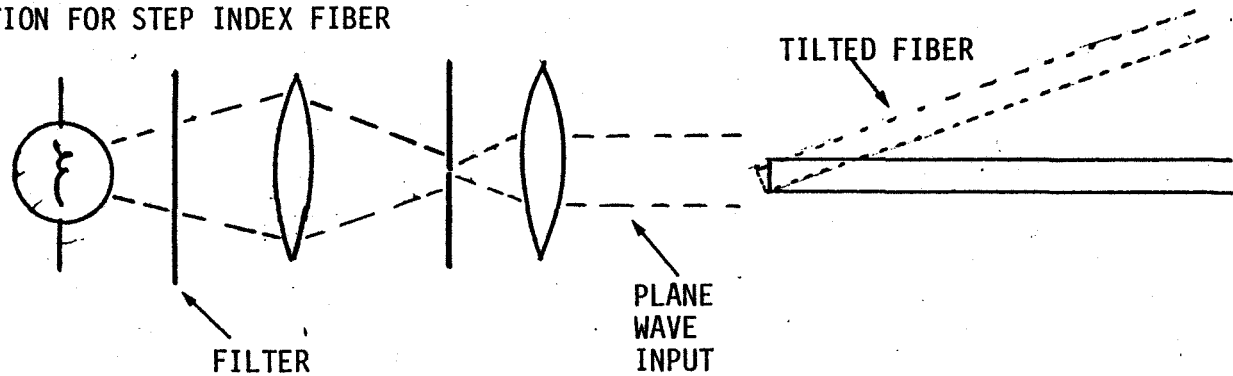
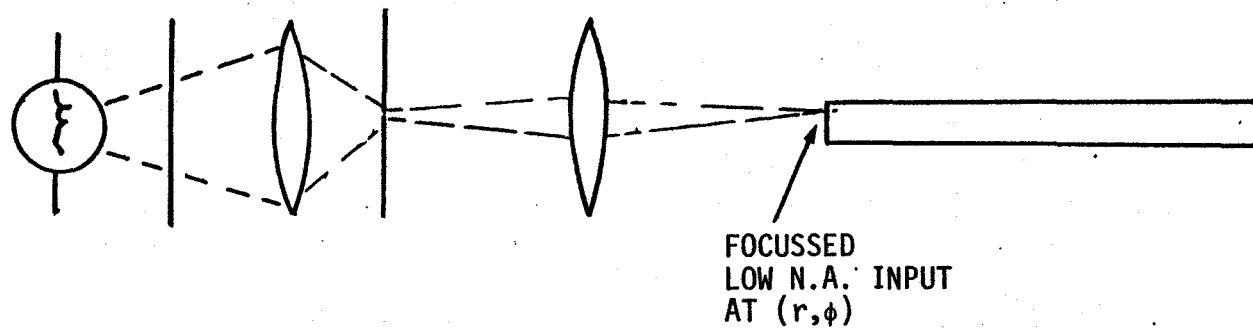


FIG. 21 (c) MODAL DEPENDENCE OF ATTENUATION FOR GRADED INDEX FIBER



relationship between the principal mode number and the input angle of the plane wave. For a graded index fiber a particular mode group may be excited by focussing a laser spot onto the core at position (r, ϕ) .

3.2.2 Coupled Power From an LED

Although it has been demonstrated that the attenuation of an optical fiber can be lowered by reducing the input N.A., this reduction does not give any practical advantages because of the resulting large reduction of the light input power. In LEDs the incoherent light emission covers a solid angle of 2π steradians. The output radiance, i.e. the output power emitted into a unit solid angle per unit emission area (a function of ϕ unless the source is Lambertian), of a surface emitting LED is relatively low, leading to low coupling efficiency into fibers. The power coupled from an LED (assumed to be Lambertian) into a step index fiber is given by:

$$P = \pi AB (N.A.)^2 \quad (9)$$

where B is the radiance, A is the light source emission area or the fiber core area, whichever is smaller, and N.A. is the numerical aperture of the fiber. Appendix B gives the simple derivation of this formula. Thus, a step index fiber with an N.A. of 0.20 will have a coupling loss to a surface emitting Lambertian LED of about 14 dB ($-10 \log 0.22$).

For a graded index fiber, the source to fiber calculation becomes more difficult because the numerical aperture is a function of the radial distance. The coupling efficiency is a function of the graded index profile parameter. A graded index fiber with a profile given by $n(r)^2 = n(0)^2 [1 - 2\Delta (\frac{r}{a})^\alpha]$ (i.e. $\alpha = 2$, for minimum dispersion) will

theoretically collect only $\frac{1}{2}$ as much as a step index fiber having the same core size and numerical aperture.

Table 3 gives the amount of light coupled into several different fibers from a typical BNR LED (#428/46). The coupled power follows the theoretically expected values extremely well. For example, between fibers 388 and 296, there is a difference in the $(N.A.)^2$ of equation (9) of a factor of $1.8 \left(\frac{0.23}{0.17} \right)^2$ and in A, one of $2.7 \left(\frac{75}{46} \right)^2$ giving a total difference of a factor of 4.9. This agrees approximately with the difference in the coupled power. Similarly, the difference can be calculated between, say, fiber #296 and #216. In this case, as one is a graded index fiber and the other a step index, a factor of 2 must also be taken into account. It should also be noted that the unstripped coupled power for the silicone coated fibers corresponds to using the fiber as a silicone clad step index fiber with the core and cladding together as a core giving a resultant N.A. of 0.40. Fiber #296 is similar to the fiber of Fig. 17. Here again approximately six times as much light is collected by the cladding than by the core. This ratio can actually be as high as 30 in the case of the 50 μ m core fibers 388, 389. However, normal fiber bonding procedures usually strip out much of this light.

3.3 Environmental Dependence of Attenuation

A series of measurements were made of the effects of temperature and ice on the attenuation of typical BNR optical fibers. This information resulted in a change from hytrel as a coating material to silicone.

3.3.1 Hytrel Coated Fibers

For various temperatures between -40 and 60°C, the variation in

TABLE 3

POWER COUPLED FROM LED 428/46
@ 100 MA DRIVE CURRENT INTO DIFFERENT
FIBER TYPES

FIBER	PROFILE	CORE SIZE	N.A.	COUPLED POWER (CLADDING LIGHT STRIPPED)	COUPLED POWER UNSTRIPPED
388	GRADED (SILICONE COATED)	46 μm	0.17	20.0 μW	570 μW
389	"	45 μm	0.18	21.0 μW	600 μW
296 (a)	"	87 μm	0.23	103 μW	676 μW
(b)	"	"	"	95 μW	660 μW
(c)	"	"	"	105 μW	192 μW *
236	STEP (HYTREL COATED)	92 μm	0.26	272 μW	AUTOMATICALLY STRIPPED BECAUSE OF HYTREL
GE670	STEP, SILICONE CLAD FIBER	120 μm	0.40	-	620 μW

* Bonded with epoxy to an LED ie. partially stripped

the light output power was monitored for six BNR 7-2-B fibers (Hytre1 coated, 150 μm O.D., 75 μm core, graded index, 0.22 N.A.) with various lengths (100-500 m). An environmental chamber was used for the test and a thermocouple recorded the temperature on a strip chart recorder. Since the tests sometimes lasted days, the intensity variation of the LED light source was monitored with the use of an optical fiber access coupler. Measurement error of the attenuation variation was approximately 0.1 dB/km for most of the tests.

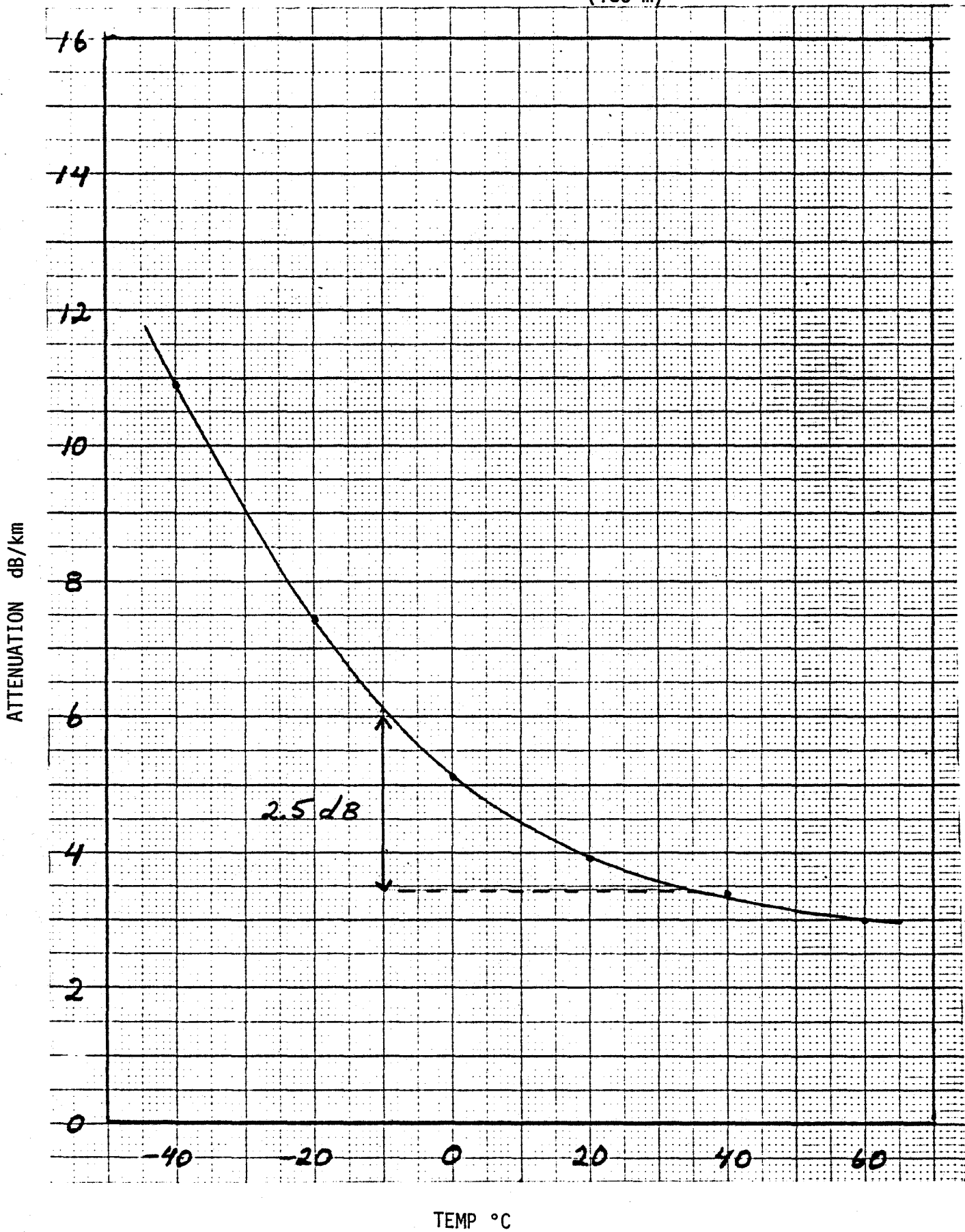
Typically, a 1.5 dB/km increase was observed at the operating temperature of -10°C relative to 35°C for the fibers with long lengths (approx. 500 m). Similarly, a 2-3 dB/km increase was observed for the short lengths (less than 200 m) between the same temperatures. Typical results are shown in Figs. 22 and 23. The length dependence of the attenuation variation is interpreted as being due to lossy modes (leaky and higher order modes) which are sensitive to the microbending losses enhanced at the low temperatures.

Temperature cycling was done on two 500 m lengths of hytre1 coated 7-2-B fiber between -40°C and 60°C . After the 10 cycle test (approximately 30 hours), no changes in the attenuation or hysteresis effects were observed. As shown in Fig. 24, the light output power followed the temperature variation repetitively except for a slight delay due to the time required to reach an equilibrium state.

The change in the attenuation of cabled 7-2-B fibers with temperature was also measured. It was determined that not only does cabling itself increase the attenuation but it can also enhance the temperature

FIG. 22

ATTENUATION VS TEMP. FIBER #197
(183 m)



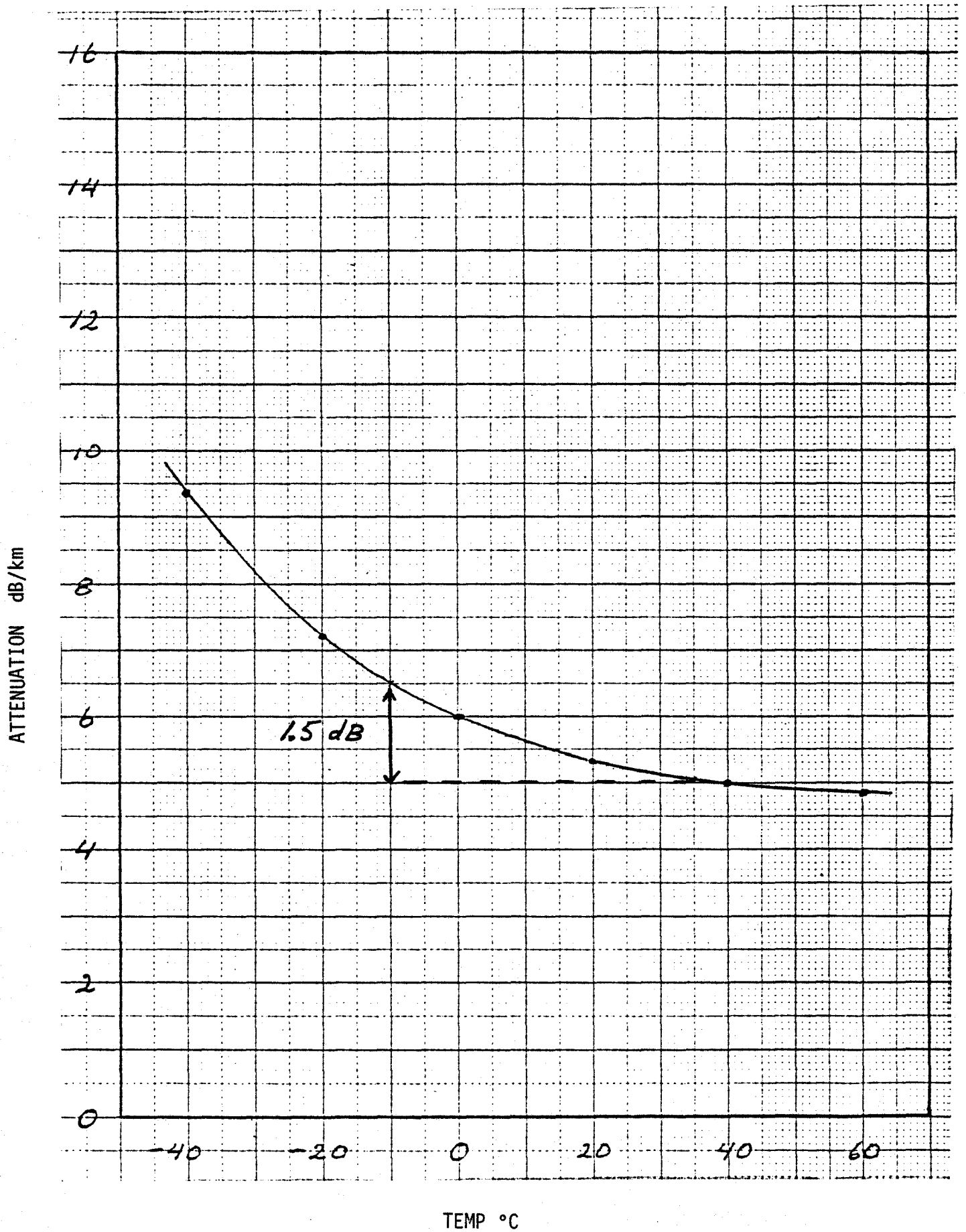
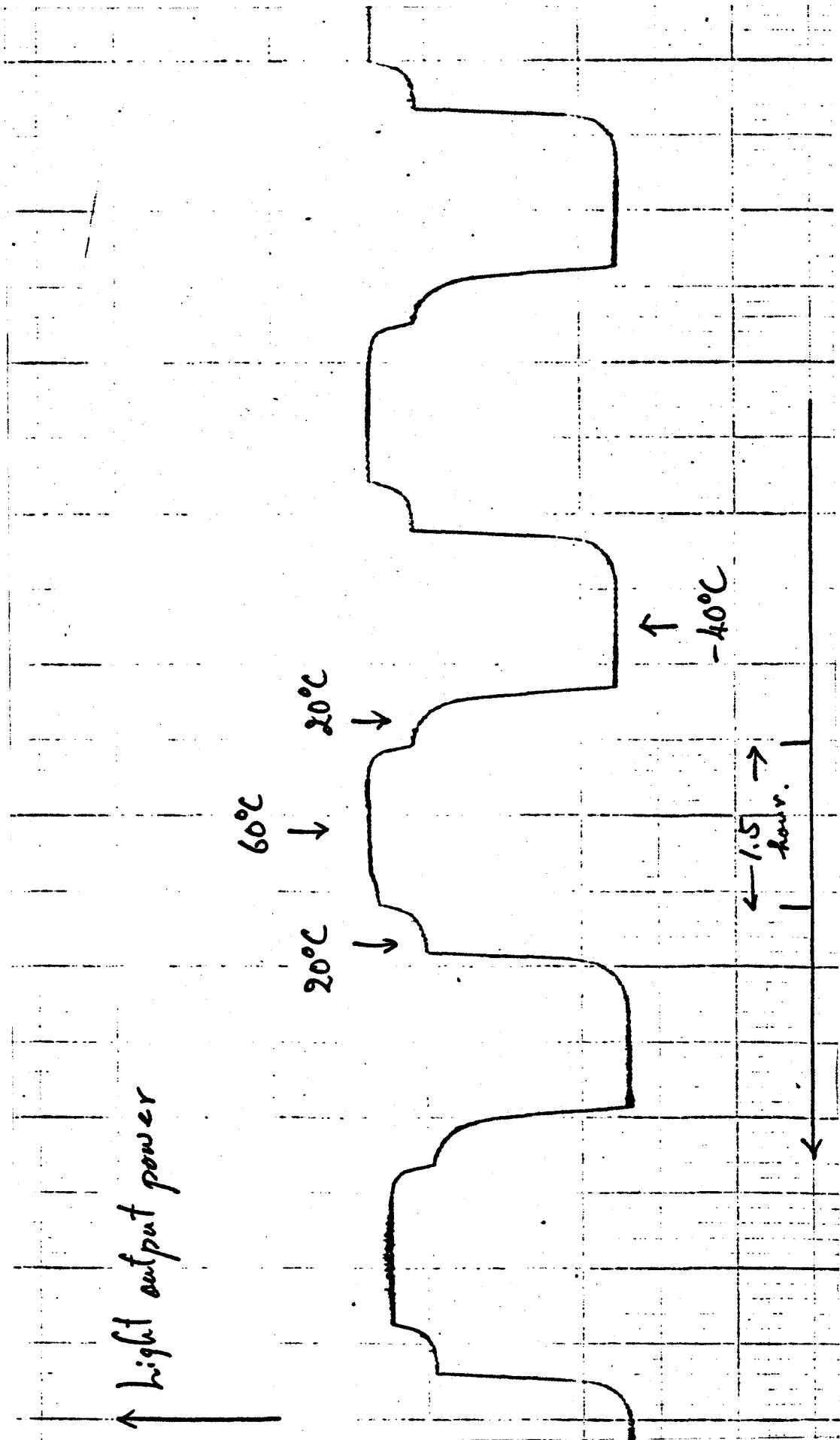


FIG. 24

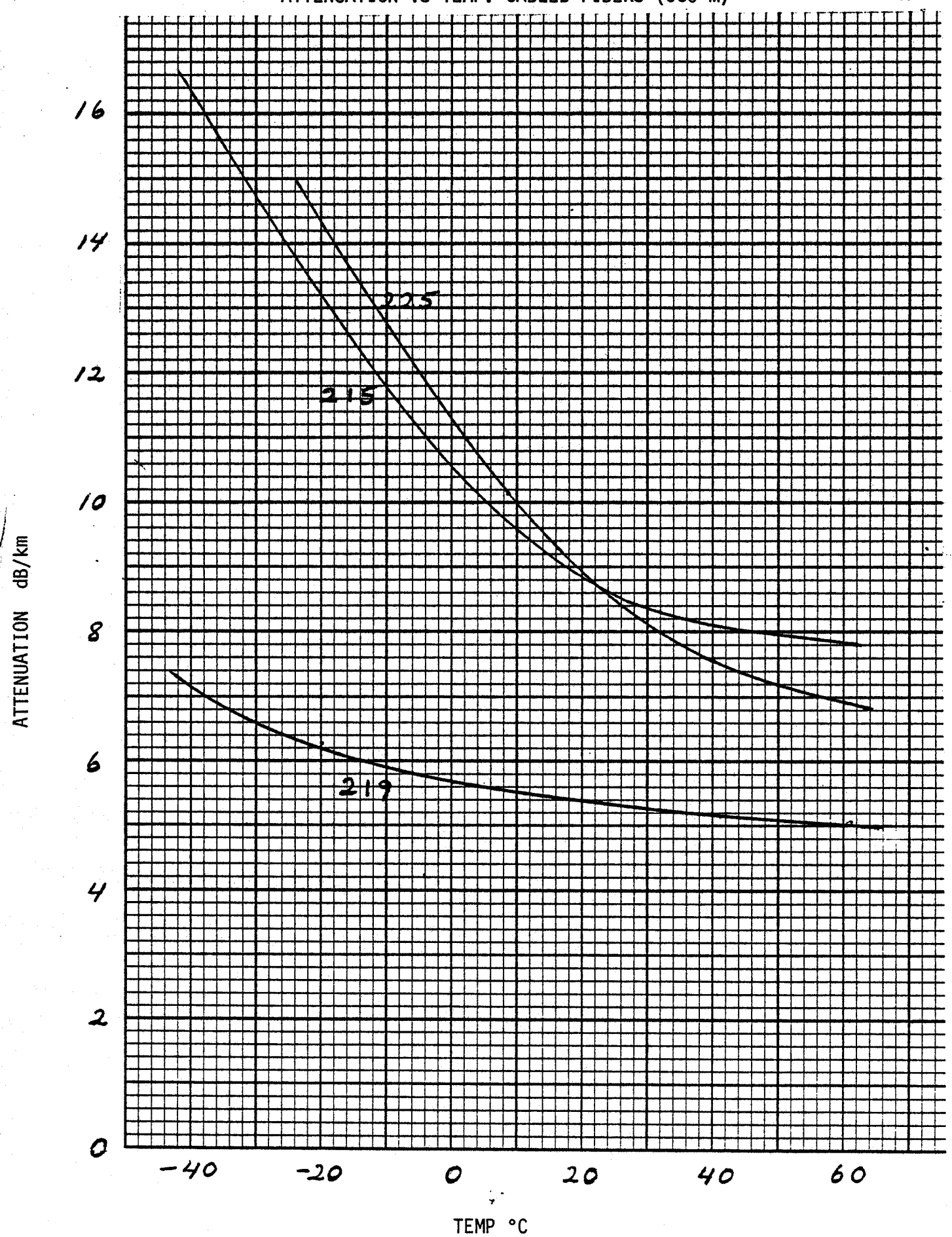
FIBER OUTPUT VS TEMP. CYCLE



(9)
effects. In Fig. 25 the attenuation as a function of the environmental temperature is shown for three 530 m lengths of cabled fiber (215, 219, and 225). Fibers 215 and 225 both of which had large attenuation increases due to cabling (2.5 and 2.2 dB/km increases compared with an average increase for 6 fibers of 1.7 dB/km) show an attenuation increase of over 3.5 dB/km at -10°C relative to 35°C , whereas cabled fiber 219 which had a negligible attenuation increase due to cabling shows an attenuation variation of less than 1 dB/km within the same temperature range. Typical attenuation variations of uncabled fibers within this range had been found to be approximately 1.5 dB/km. Thus, it was concluded that if the attenuation increase due to cabling is minimized the temperature dependent attenuation due to cabling can be too.

The effects of ice on the attenuation of hytrel coated 7-2-B fibers was tested. In one test, loose loops of a 500 m fiber were immersed in tap water and were frozen at -10°C . For this test the thermocouple was located in the ice. The attenuation increased to over 1000 dB/km. Using a helium-neon laser it was observed that the loss was uniform along the full length and was not due to breakage of the fiber or to isolated stress points. Also, the original attenuation was recovered after the ice melted.

In another ice test with 7-2-B hytrel coated fibers, a short duplex cable (2 fibers in a HDPE tube) (30 M) was filled with water and frozen and the temperature reduced to -20°C . The attenuation increase resulting from the freezing is clearly demonstrated in Fig. 26. Extrapolating to a 1 km length the attenuation increase was estimated to be over 100 dB/km.



FREEZE TEST
DUPLX CABLE (30 m)

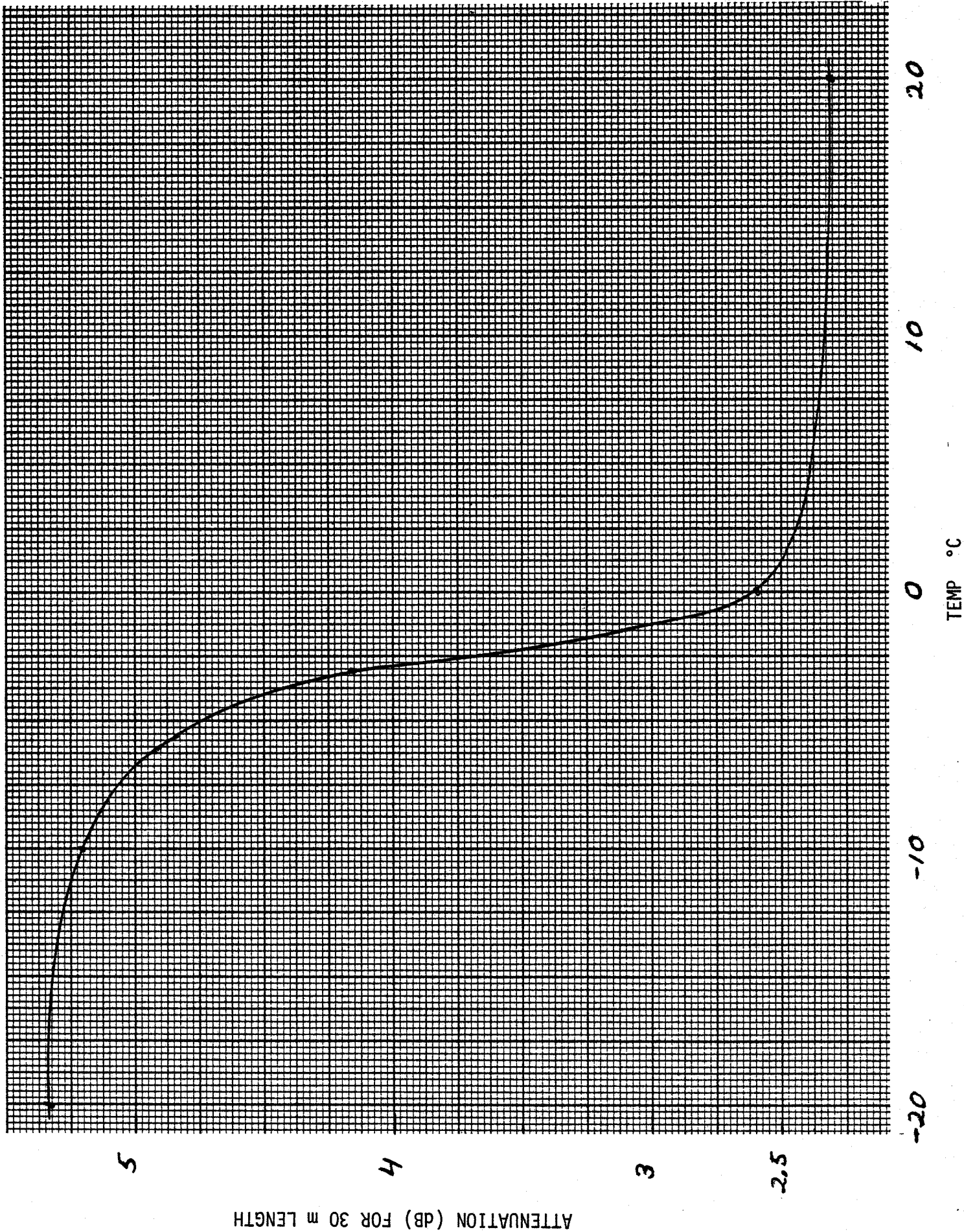


FIG. 26

ATTENUATION (dB) FOR 30 m LENGTH

TEMP °C

3.3.2 Silicone Coated Fibers

A few experiments done with silicone coated fibers showed no increases in attenuation due to changes in temperature from -40°C to 60°C . Although silicone has a large temperature coefficient of expansion, it is very soft and does not seem to cause the large microbending losses of fibers coated with hytrel or nylon.

Silicone coated fibers, however, do show an increased attenuation upon freezing in ice but the effect is much less than with the hytrel fibers. Fig. 27 shows the attenuation variation of a 1 km length of silicone coated fiber in a tray of water which was frozen and cooled further to a temperature of -40°C . It can be seen that there is no increase upon freezing of the water and reducing the temperature to $\sim -4^{\circ}\text{C}$. Only upon further reduction in temperature was an increased loss observed.

FIG. 27

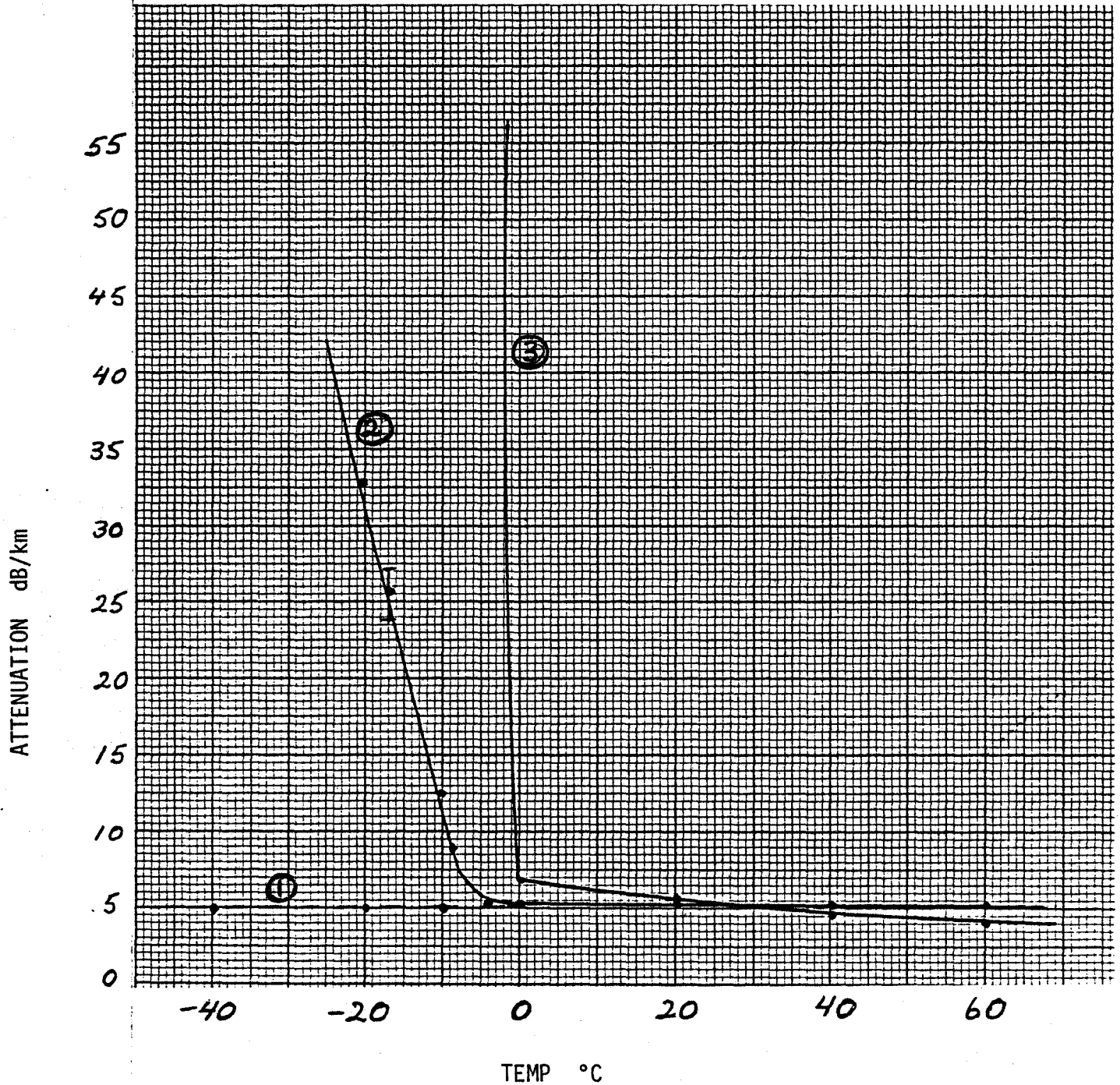
ATTENUATION VS TEMP. OF:

A) SILICONE COATED FIBER #177
(280 m, GRADED INDEX, 75 μm CORE, 150 μm O.D., 0.21 N.A.)

- (1) IN AIR
- (2) IN ICE

B) HYTREL COATED FIBER #203 (840 M)

- (3) IN ICE



CHAPTER 4

CONCLUSION

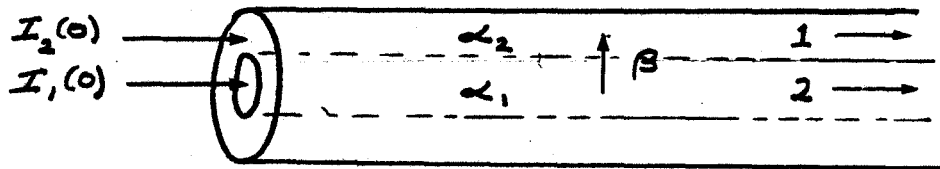
The subjects of attenuation and spectral loss were reviewed in this project along with some of the more important parameters affecting their measurement. The new techniques which were developed during the work term, such as the use of a fiber "pigtail" as a mode equalizer and the direct display method for spectral attenuation, are still in use at BNR. Silicone has been used as a protective jacket for the optical fiber since the early measurements were done on temperature dependence of loss.

This paper is not a complete study of optical fiber attenuation. Other effects which were not covered include intrinsic losses caused by 1) microbending (minute bends), 2) macrobending (gradual bends), 3) radiation damage and 4) structural defects such as changes in core shape or size at different points along the fiber. The last cause listed above can be studied most easily by Optical Time Domain Reflectometry (OTDR) which analyzes backscattered light returned from a long section of fiber. Work is presently continuing in this area.

APPENDIX A

A Calculation of the Relative Amounts of
Core and Cladding Light in a Silicone
Coated Optical Fiber vs. Fiber Length

Consider the transmitting fiber shown below:



where $I_1(0)$ is the light in the core at position $z = 0$.

$I_2(0)$ is the light retained by the cladding at $z = 0$.

α_1 represents the loss of the core due to all causes except transfer to the cladding.

α_2 represents the cladding loss.

β represents the loss from the core which is retained by the cladding.

The core loss rate equation then becomes:

$$\frac{dI_1}{dz} = -(\alpha_1 + \beta)I_1$$

or

$$I_1(z) = I_1(0)e^{-(\alpha_1 + \beta)z} \quad (A1)$$

The cladding loss rate equation is then:

$$\frac{dI_2}{dz} = \beta I_1 - \alpha_2 I_2$$

which becomes

$$\begin{aligned} I_2(z) &= e^{-\alpha_2 z} \left[\beta \int e^{\alpha_2 z} I_1(z) dz + C \right] \\ &= e^{-\alpha_2 z} \left[\beta I_1(0) \frac{e^{(\alpha_2 - \alpha_1 - \beta)z}}{\alpha_2 - \alpha_1 - \beta} + C' \right] \end{aligned}$$

But

$$I_2(0) = \frac{\beta I_1(0)}{\alpha_2 - \alpha_1 - \beta} + C'$$

$$\therefore I_2(z) = e^{-\alpha_2 z} \left[\frac{\beta I_1(0)}{\alpha_2 - \alpha_1 - \beta} \left(e^{(\alpha_2 - \alpha_1 - \beta)z} - 1 \right) + I_2(0) \right]$$

$$\begin{aligned} &= \frac{\beta I_1(0)}{\alpha_2 - \alpha_1 - \beta} \begin{pmatrix} e^{-(\alpha_1 + \beta)z} & e^{-\alpha_2 z} \\ & -e^{-\alpha_2 z} \end{pmatrix} + I_2(0) e^{-\alpha_2 z} \\ &= \frac{\beta' I_1(0)}{\alpha_2' - \alpha_1' - \beta'} \begin{pmatrix} 10 & \frac{-(\alpha_1' + \beta')z}{10} \\ & -10 & e^{-\alpha_2' z} \end{pmatrix} + I_2(0) 10 \frac{e^{-\alpha_2' z}}{10} \end{aligned}$$

where α_1' , α_2' , β' are now in dB/km.

Changing the variables slightly once more this becomes:

$$I_2(z) = \beta' \frac{I_1(0)}{k_2 - k_1} \begin{pmatrix} 10 & \frac{-k_1 z}{10} \\ & -10 & \frac{-k_2 z}{10} \end{pmatrix} + I_2(0) 10 \frac{e^{-k_2 z}}{10}$$

(A2)

where k_1 = attenuation of core in dB/km

k_2 = attenuation of cladding in dB/km

β' = amount of light lost from the core to the cladding in dB/km

z = km

To get:

$$k_1 (= \alpha_1 + \beta) \longrightarrow \text{measure } I_1(z) \text{ and use equation (A1)}$$

$$k_2 = \alpha_1 \longrightarrow \text{measure } I_2(z) \text{ with } I_1(0) = 0 \text{ and } I_2(0) \neq 0$$

(a method for doing this is described on page of the text.)

$$\beta' \longrightarrow \text{measure } I_2(z) \text{ with } I_1(0) = 0 \text{ and } I_2(0) = 0$$

Example

For the fiber of figure 17, the following measurements were taken:

$$k_1 \approx 3 \text{ dB/km}$$

$$k_2 \approx 20 \text{ dB/km}$$

$$I_2(0) \approx 6 I_1(0)$$

equation (A2) becomes:

$$I_2(1\text{km}) = \frac{\beta' I_1(0)}{20 - 3} \left(10^{-0.3} - 10^{-2} \right) + 6 I_1(0) 10^{-2}$$

$$I_2(2\text{km}) = \frac{\beta' I_1(0)}{20 - 3} \left(10^{-0.6} - 10^{-4} \right) + 6 I_1(0) 10^{-4}$$

as the length of fiber increases equation (A2) tends to (if $\alpha_2 \gg \alpha_1$):

$$I_2(z) \approx \frac{\beta' I_1(0)}{k_2 - k_1} \left(10^{\frac{-k_1 z}{10}} \right) \quad (\text{A3})$$

$$\text{but } I_1(z) = I_1(0) 10^{\frac{-k_1 z}{10}}$$

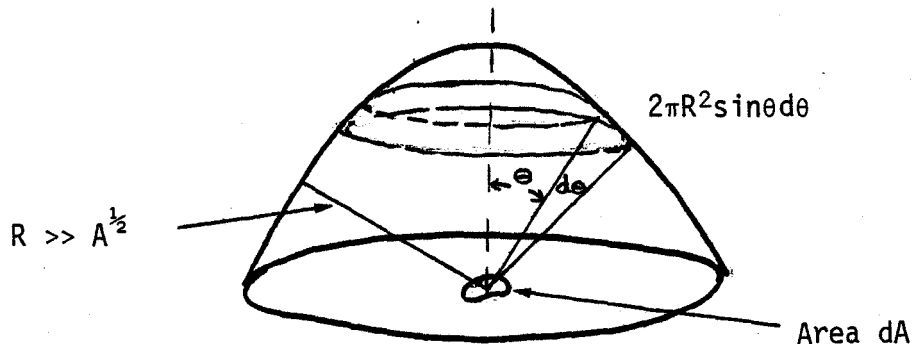
$$\text{so } \frac{I_2}{I_1} \text{ becomes: } \gamma = \frac{I_2}{I_1} = \frac{\beta'}{k_2 - k_1} = \text{constant}$$

APPENDIX B

A Calculation of the Light Collected by
a Fiber from a Lambertian LED

Suppose the LED is a flat diffuse source of area A emitting with a radiance B in watts $\text{ster}^{-1}\text{cm}^{-2}$.

Consider a small area dA of the LED radiating into a hemisphere of 2π steradians as shown below:



The incremental ring area is $2\pi R \sin \theta \times R d\theta$, and subtends a solid angle of $2\pi \sin\theta d\theta$ steradians.

The radiation intercepted by this ring is:

$$dP = J_{\theta} \times (2\pi \sin\theta d\theta)$$

where J_{θ} is the radiant intensity of the LED source in watts/steradian at angle θ .

$$\begin{aligned} &= J_{\theta} \cos\theta (2\pi \sin\theta d\theta) \\ &= B dA \cos\theta (2\pi \sin\theta d\theta) \end{aligned}$$

$$\left(\text{here } B_{\theta} = \frac{J_{\theta} \cos\theta}{dA \cos\theta} = B \text{ (const)} \right)$$

For a step index fiber with an acceptance angle of θ_0 , the power collected by the fiber is then:

$$\begin{aligned}
 P &= \int_{\text{area}} \int_0^{\theta_0} 2\pi B \sin\theta \cos\theta d\theta dA \\
 &= 2\pi AB \left[\frac{\sin^2\theta}{2} \right]_0^{\theta_0} = \pi AB \sin^2\theta_0 \\
 &= \pi AB (\text{N.A.})^2
 \end{aligned}$$

REFERENCES

- (1) Barnoski, M.K., and Personick, S.D., "Measurements in Fiber Optics", Proc. IEEE, Vol. 66, No. 4, April 1978, pp. 429-441.
- (2) Conradi, J., "Planar Germanium Photodiodes", Applied Optics, Vol. 14, No. 8, August 1975, pp. 1948-1952.
- (3) Duck, G., and Abe, K., "Direct Display of Optical Fiber Spectral Attenuation", Internal BNR Memo, September 1977.
- (4) Luther-Davies, B., et al, "Evaluation of Material Dispersion in Low Loss Phosphosilicate Core Optical Fibers", Optics Communications, Vol. 13, No. 1, January 1975, pp. 84-88.
- (5) Horiguchi, M., "Spectral Losses of Low OH Content Optical Fibers", Electronics Letters, Vol. 12, No. 12, June 10, 1976, pp. 310-312.
- (6) Duck, G., and Abe, K., "Attenuation of Phosphorus Doped Silica Core Fiber", Internal BNR Memo, June 1977.
- (7) Inada, K., et al, "'Silfa' Silicone Clad Optical Fiber", Fujikura Technical Review, 1977, pp. 44-55.
- (8) Kaiser, P., et al, "Spectral Losses of Unclad Vitreous Silica and Soda-Lime-Silicate Fibers", Journal of the Optical Society of America, Vol. 63, No. 9, September 1973, pp. 1141-1148.
- (9) Duck, G., and Abe, K., "Foet 5 Cable Attenuation Measurements", Internal BNR Memo, July 1977.

REFERENCES NOT CITED

- Campbell, L., "Fiber and Integrated Optics", Vol. 1, No. 1, 1977, Crane, Russak and Co. Inc., pp. 21-37.
- Duck, G., "Foet Meeting", Internal BNR Memo, September 1977.
- Giallorenzi, T., "Optical Communications Research and Technology: Fiber Optics", Proc. IEEE, Vol. 66, No. 7, July 1978, pp. 744-780.
- Gloge, D., and Marcetili, E., "Multimode Theory of Graded-Core Fibers", Bell System Technical Journal, November 1973, pp. 1563-1578.
- Kaiser, P., "Drawing - Induced Coloration in Vitreous Silica Fibers", Journal of the Optical Society of America, Vol. 64, No. 4, April 1974, pp. 475-481

McGovern, P., Laser Focus Buyer's Guide 1976, February Issue.

Payne, D., and Gambling, W., "Preparation of Water-Free Silica-Based Optical Fiber Waveguide", Electronics Letters, Vol. 10, No. 16, August 8, 1974, pp. 335-336.

Payne, D., and Gambling, W., "Zero Material Dispersion in Optical Fibers", Electronics Letters, Vol. 11, No. 8, April 17, 1975, pp. 176-178.

Shimada, S., et al, "Progress in Optical Fiber Transmission Technology", Japan Telecommunications Review, April 1977, pp. 86-96.